STRUCTURE FUNCTIONS AT SMALL X

J. BLÜMLEIN, DESY-ZEUTHEN

1) INTRODUCTION
2) EXTRAPOLATION OF AP TOWARDS SMALL x & HO RESULTS
3) RESUMMING SMALL x EFFECTS:
   - BFKL equation
   - THE ONSET OF SHADOWING
   - $k_\perp$ FACTORIZATION & F_L, F_2
4) HERA PROSPECTS
   - WAYS TO EXTRACT STRUCTUREFUNCTIONS
   - UNFOLDING PARTON DISTRIBUTIONS, $x\overset{(-)}{q}_i$, xG
   - α_s & Λ_{QCD}
5) FIRST RESULTS FROM HERA.

E. LANSING, 5/6/93

1 INTRODUCTION

DIS:

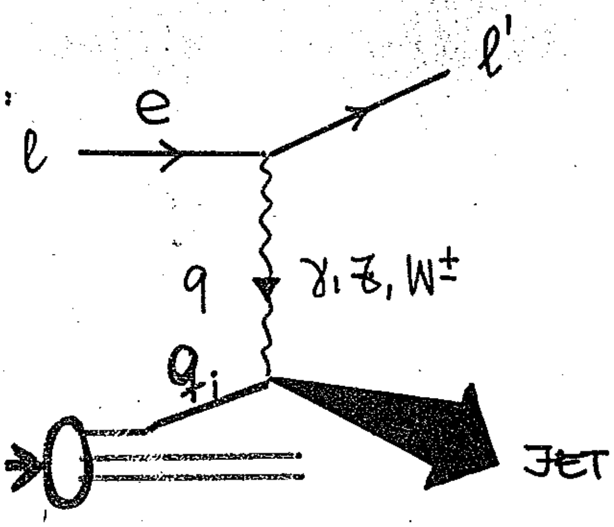

$$\boxed{\begin{aligned} x &= \frac{-q^2}{2qp} \\ y &= \frac{qp}{\ell p} \end{aligned}} \qquad ; \quad -q^2 = Q^2$$

FIXED TARGET : $x \gtrsim 5 \cdot 10^{-3} \ldots 10^{-2}$; $y \lesssim .7$, $Q^2 \lesssim 200\,\mathrm{GeV}^2$

HERA : $x \gtrsim 10^{-4}$ at $Q^2 \sim 10\,\mathrm{GeV}^2$

$x \sim 0.5$ at $Q^2 \sim$ sev. $10^4\,\mathrm{GeV}^2$.

PROBLEMS : – EVOLUTION DYNAMICS @ SMALL x

- $\alpha_s \ln \frac{1}{x} \sim 1$
- HIGH GLUON DENSITIES → RECOMBINATION !?

– PARTON INTERPRETATION OF STRUCTURE FUNCTIONS ?

– WHERE DO WE STAND QUANTITATIVELY ?

K3

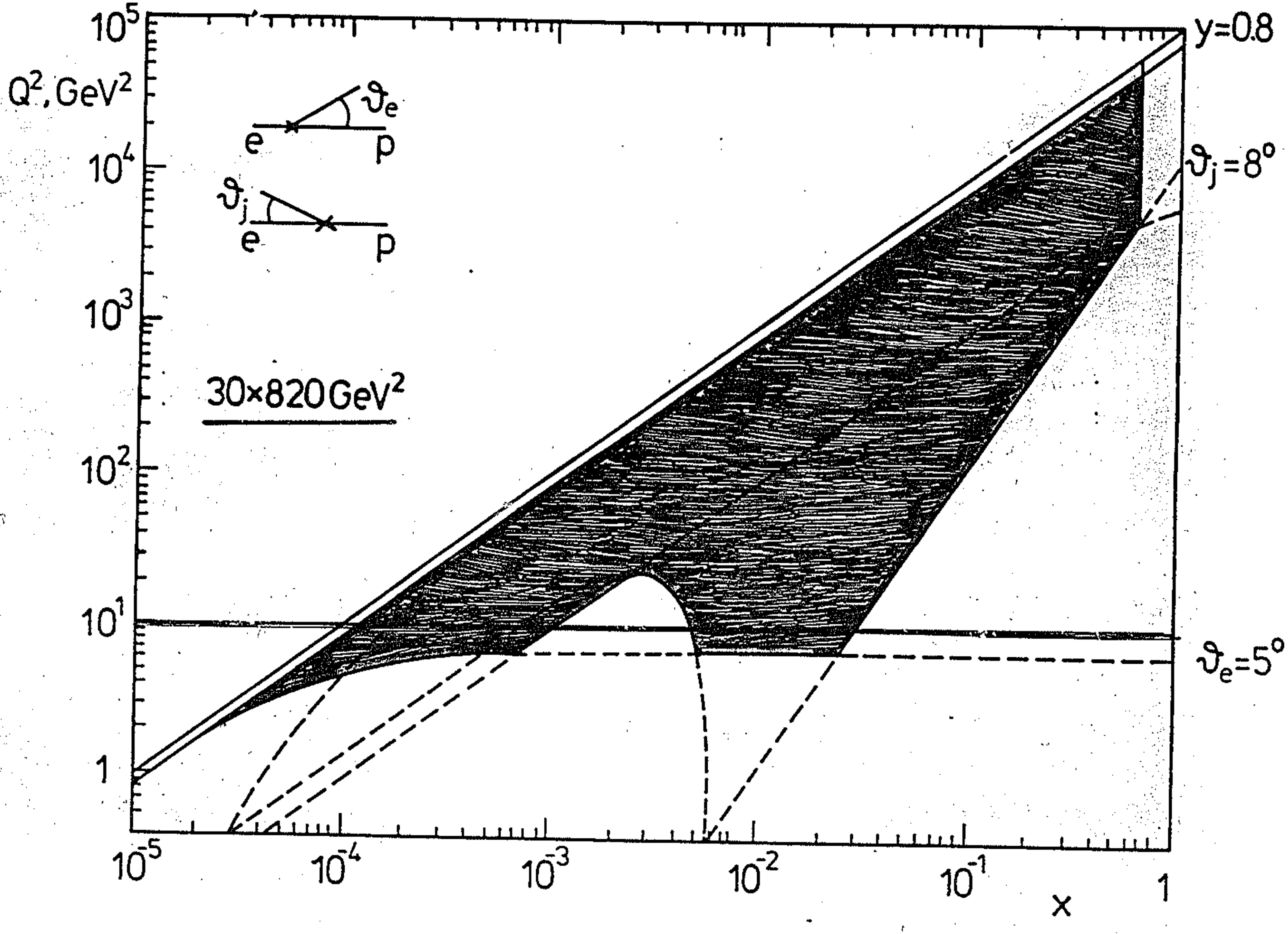

Q^2, GeV^2
10^5
10^4
10^3
10^2
10^1
1
10^{-5}
10^{-4}
10^{-3}
10^{-2}
10^{-1}
1
x
ϑ_e
e
p
ϑ_j
e
p
30×820 GeV^2
y=0.8
$\vartheta_j=8^\circ$
$\vartheta_e=5^\circ$

K4

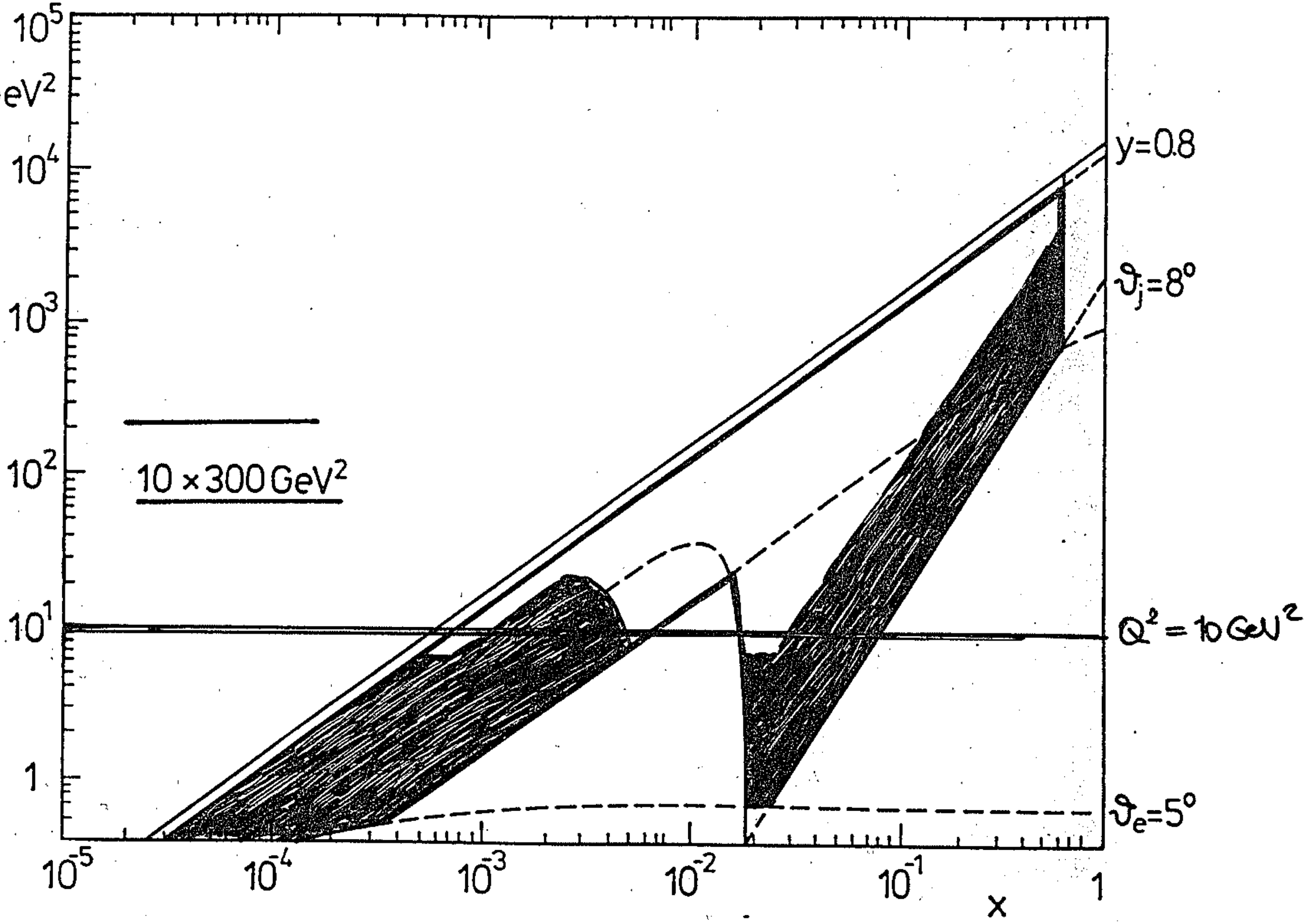

Q^2, GeV^2
10^5
10^4
10^3
10^2
10^1
1
$10 \times 300\,GeV^2$
10^{-5}
10^{-4}
10^{-3}
10^{-2}
10^{-1}
1
x
y=0.8
$\vartheta_j = 8°$
$Q^2 = 10\,GeV^2$
$\vartheta_e = 5°$

2. EXTRAPOLATION OF THE AP EQUATIONS TO SMALL x

CONSIDER THE GLUON DISTRIBUTION: $\quad q_s(x) \ll G(x)$

$$\mathbb{G}(x,Q^2) := x\,G(x,Q^2)$$

$$\frac{d\mathbb{G}(x,Q^2)}{d\ln Q^2} = \frac{\alpha_s(Q^2)}{2\pi}\int_x^1 \frac{dx'}{x'}\Big[\underset{\substack{\uparrow\\ \mathrm{LO}}}{6}-\underset{\substack{\uparrow\\ \mathrm{NTLO}}}{\frac{61}{9}N_f\frac{\alpha_s}{2\pi}}\Big]\frac{x^2}{x'^2}\,\mathbb{G}(x',Q^2)$$

DF.: $\quad y = \frac{8N_c}{\beta_0}\ln\frac{1}{x} \quad , \quad \xi = \ln\ln\frac{Q^2}{\Lambda^2}$

$$\boxed{\begin{array}{lr} \dfrac{\partial^2\mathbb{G}(y,\xi)}{\partial y\,\partial\xi} = \dfrac{1}{2}\,\mathbb{G}(y,\xi) & \mathrm{LO} \\[2ex] \dfrac{\partial\,\mathbb{G}(y,\hat{\xi})}{\partial y\,\partial\hat{\xi}} = \dfrac{1}{2}\,\mathbb{G}(y,\hat{\xi}) & \mathrm{NTLO} \end{array}}$$

$$\hat{\xi} = \xi + f(\xi) \;;\; f'(\xi) = -\left[\frac{\beta_1}{\beta_0}\xi e^{-\xi} + \frac{61}{62}\frac{2N_f}{\beta_0}e^{-\xi}\left(1-\frac{\beta_1}{\beta_0}\xi e^{-\xi}\right)^2\right]$$

SOLUTION:

$$\mathbb{G}(y,\overset{(\wedge)}{\xi}) = \sum_{\nu=0}^{\infty}\left\{A_\nu\left(\frac{2\overset{(\wedge)}{\xi}}{y}\right)^{\nu/2} + B_\nu\left(\frac{y}{2\xi}\right)^{\nu/2}\right\}$$

- $\mathbb{G}(y,\xi)$ GROWS FASTER THAN A POWER OF $\ln\frac{1}{x}$ FOR $x\to 0$
- $\mathbb{G}(y,\hat{\xi}) < \mathbb{G}(y,\xi)$

AP EQUATIONS:

$$\frac{d f^a(x, Q^2)}{d \ln Q^2} = P\left(x, \frac{\alpha_s(Q^2)}{2\pi}\right)_{ab} \otimes f_b(x, Q^2)$$

$$P\left(x, \frac{\alpha_s}{2\pi}\right)_{ab} = \frac{\alpha_s}{2\pi}\left\{ P^0_{ab}(x) + \frac{\alpha_s}{2\pi} P^1_{ab}(x) + \dots \right\}$$

$$x \ll 1$$

	1ST ORDER	2nd ORDER
FF	$C_F \frac{1+x^2}{1-x}$	$\frac{1}{x} 2N_f T_R C_F \left(+\frac{20}{9}\right)$
FG	$2N_f T_R \left[x^2 + (1-x)^2\right]$	$\frac{1}{x} 2N_f T_R C_G \left(+\frac{20}{9}\right)$
GF	$C_F \frac{1}{x}\left[1 + (1-x)^2\right]$	$\frac{1}{x} 2N_f T_R \left(-\frac{20}{9}\right) + C_F C_G$
GG	$2C_G\left[\frac{1}{x} + \frac{1}{1-x} - 2 + x - x^2\right]$	$\frac{1}{x} 2N_f T_R \left(-\frac{23}{9} C_G + \frac{2}{3} C_F\right)$

WU-KI TUNG

1ST & 2nd ORDER EVOLUTION

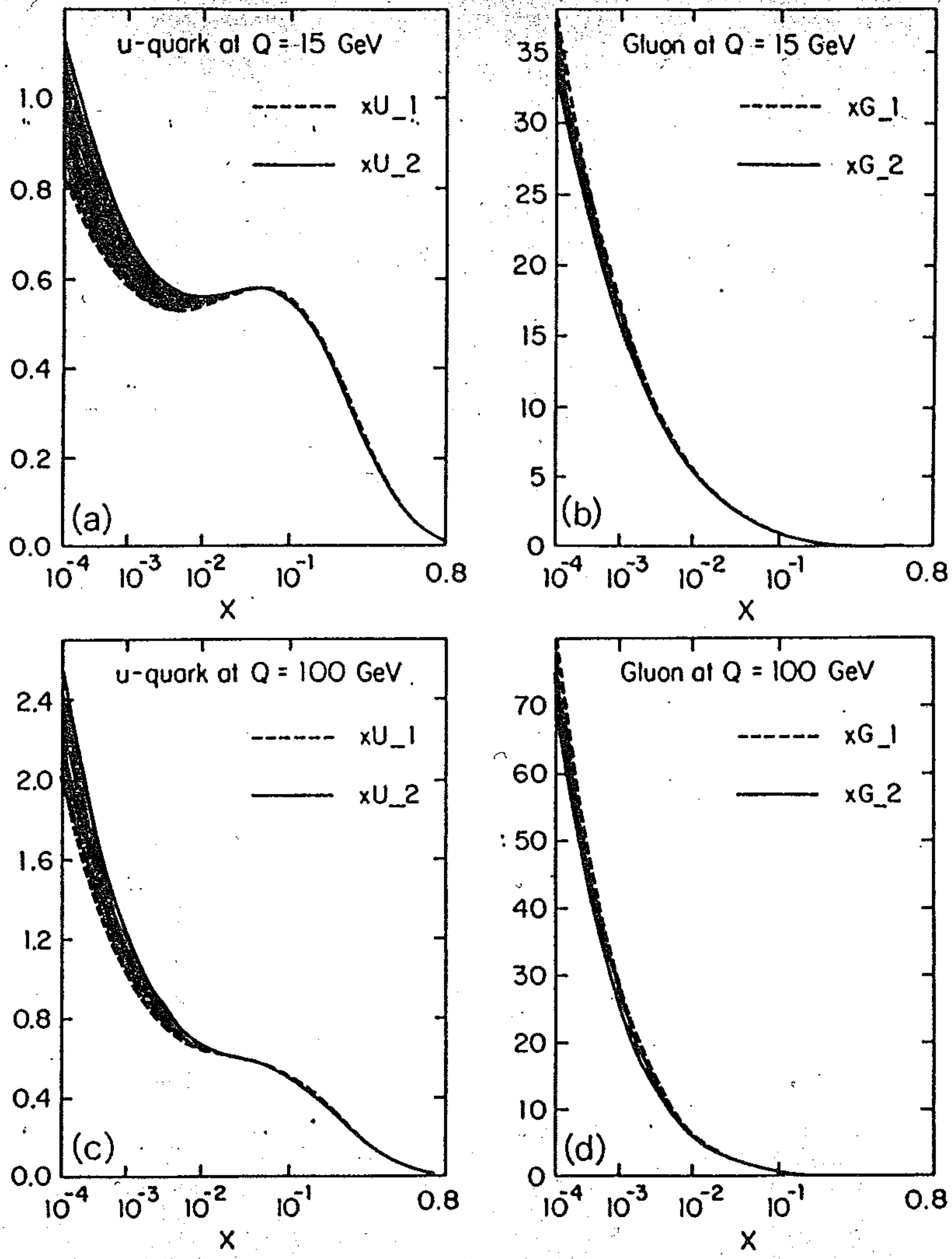

Fig. 1. Comparison of first- and second-order evolved parton distributions. Plotted are x times the probability distributions. Parton species and Q-values are as labeled. Initial distributions at $Q = 4.0$ GeV are taken from EHLQ set 1.

SCHEME DEPENDENCE

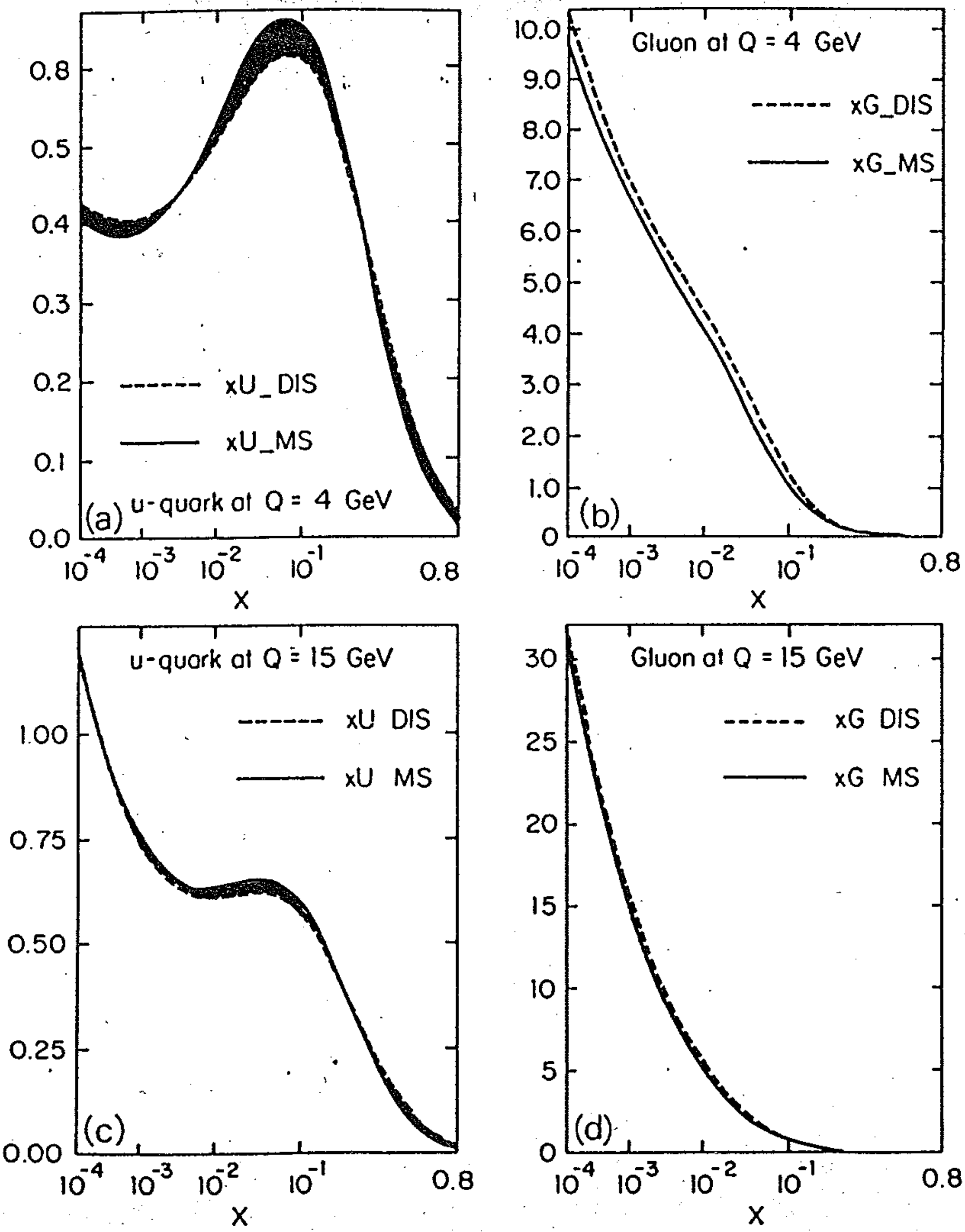

Fig. 3. Comparison of DIS-scheme and MS-bar scheme parton distributions. Plotted are x times the probability distributions. Parton species and Q-values are as labeled. Initial distributions at $Q = 4.0$ GeV are taken from EHLQ set 1.

IMPORTANCE OF HIGHER ORDER CORRECTIONS

ZIJLSTRA, VAN NEERVEN

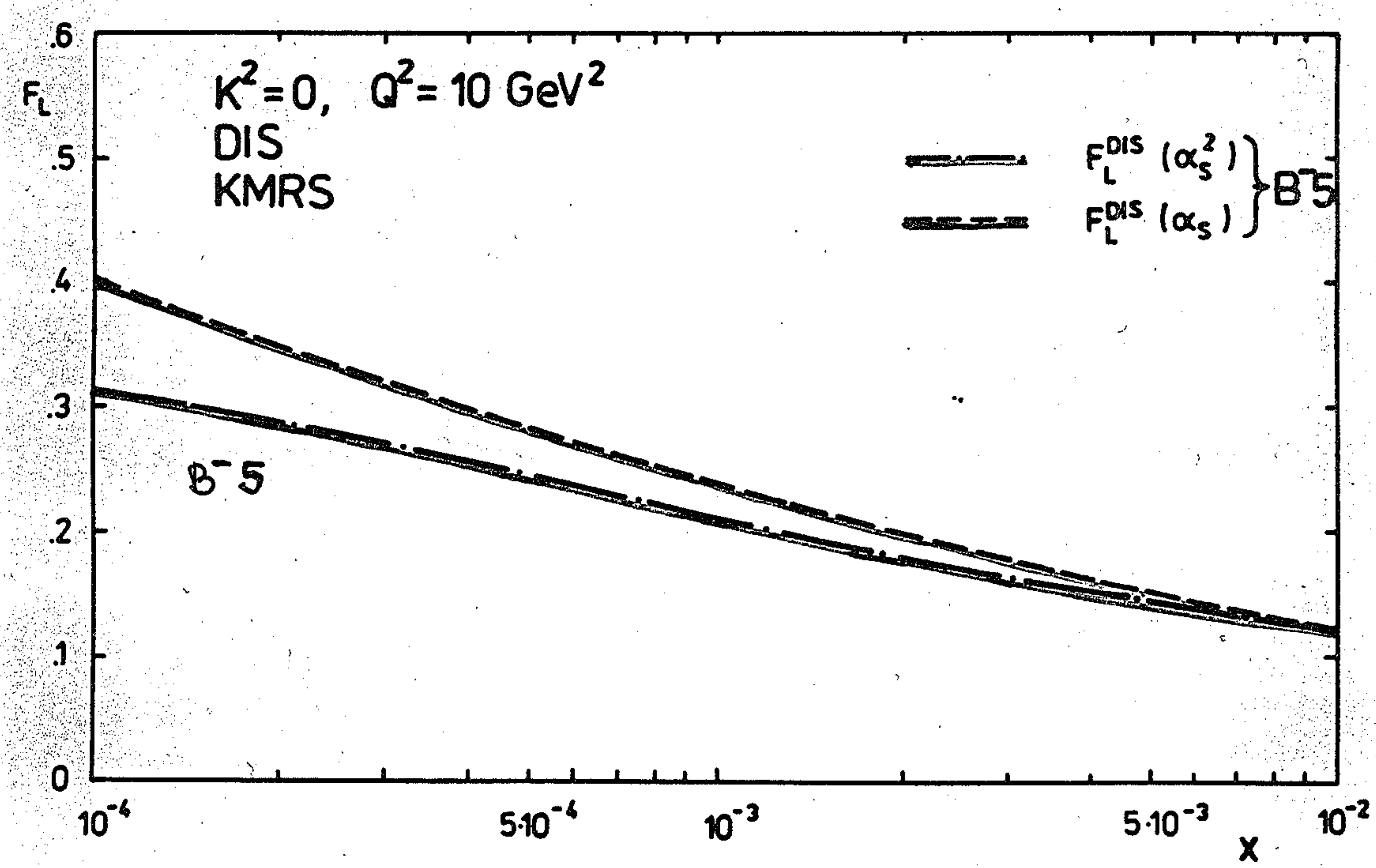

ZIJLSTRA, VAN NEERVEN

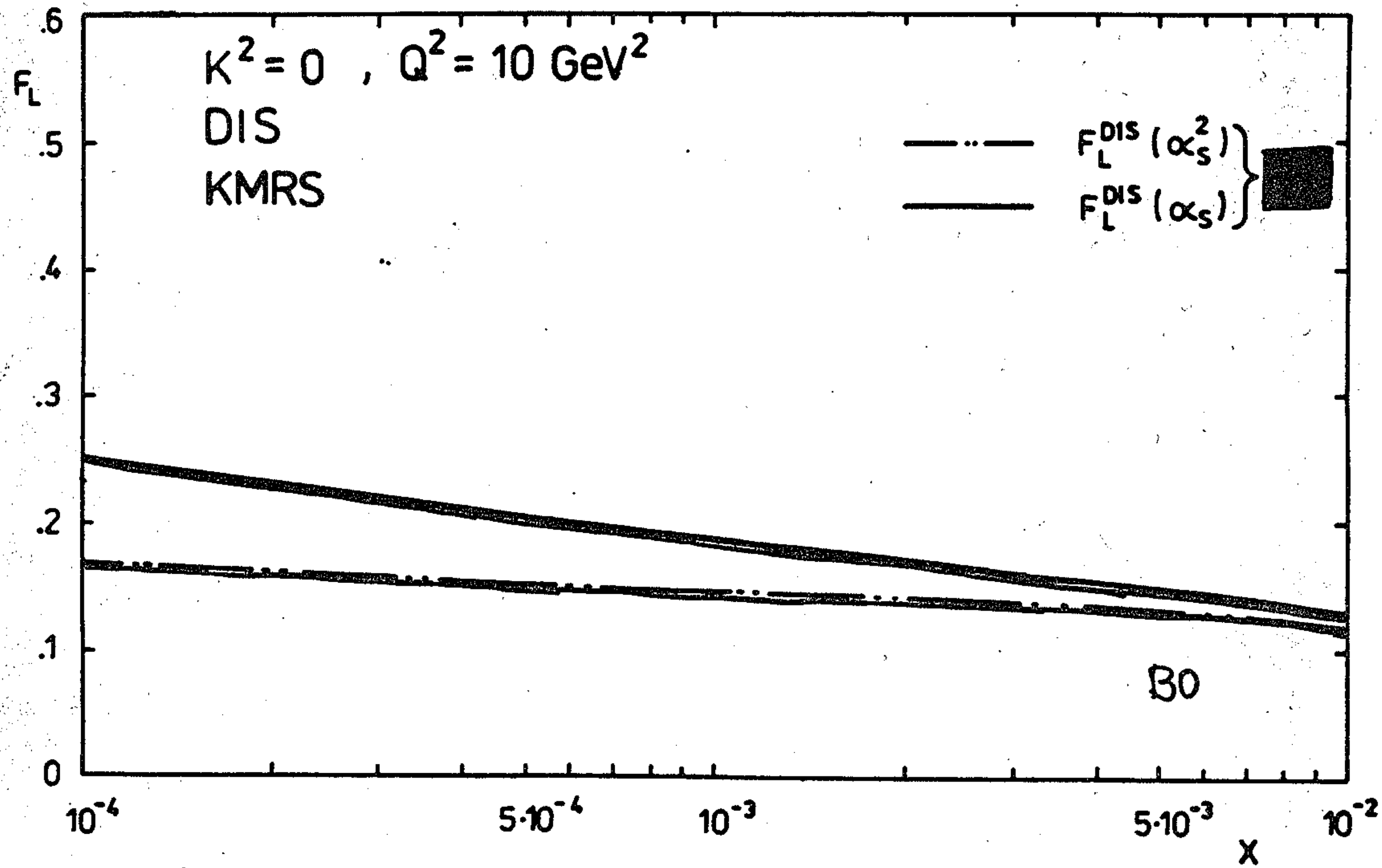

$$R^{(2)}(x,Q^2) = \frac{F_L^{(2)}(x,Q^2)}{\left(1+\frac{4M_p^2x^2}{Q^2}\right)F_2^{(1)}(x,Q^2) - F_L^{(2)}(x,Q^2)}$$

$O(\alpha_s^2)$

ZIJLSTRA, VAN NEERVE

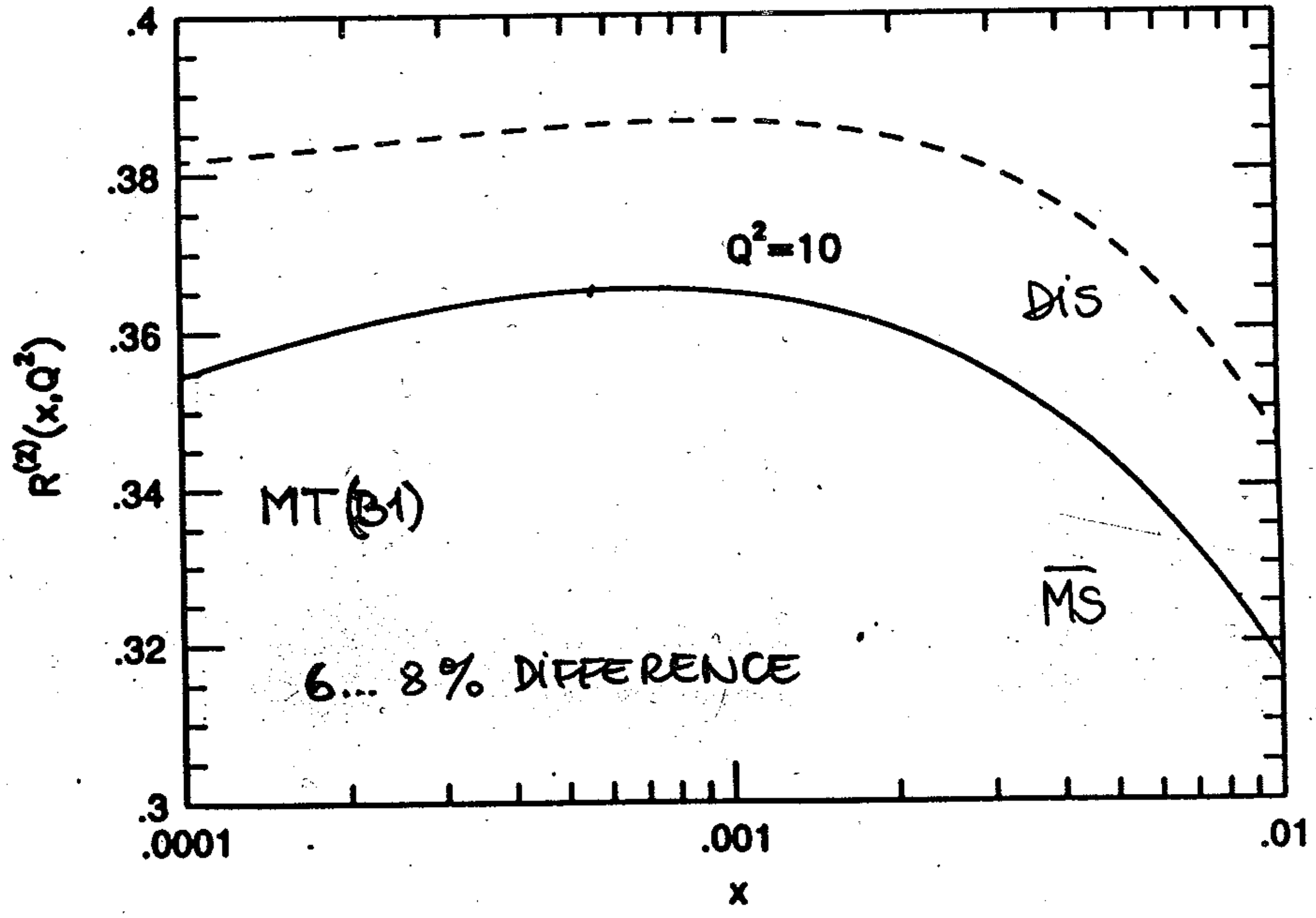

3. RESUMMING SMALL x EFFECTS

⇒ CENTRAL QUESTION.

→ RESUMMATION REQUIERES ('EVOLUTION') INTEGRAL EQUATION(S).

- BSE's, or similar eqs.

→ TO BE STRICTLY DERIVED IN QCD.

- SUMMING $\ln\frac{1}{x}$ TERMS: BFKL equation. (LIN. eq.)!
  - → FACTORIZATION?
  - → WHICH LOCAL OPERATORS ARE ENCOUNTERED? (NOT KNOWN YET.)
  - → HIGHER TWISTS ARE SUMMED <u>PARTLY</u>!

a) BFKL equation

- PARTON RECOMBINATION EFFECTS

"$G + G \to G$"

b) GLR equation

a) THE BFKL - EQUATION

FADIN, KURAEV, LIPATOV; BALITZKII

$$f(n,k^2) = \frac{1}{n-1} f_0(n,k^2) + \frac{3}{\pi}(\mathcal{L} \otimes f)(n,k^2)$$

i) $\alpha_s = \text{const.} \quad \mathcal{L} = L_1$

$$L_1 \otimes f_n = \frac{\alpha_s}{n-1}\int_{k_0^2}^{\infty} \frac{d\bar{k}^2}{\bar{k}^2} \left\{ \frac{k^2}{|\bar{k}^2 - k^2|}\left[f(n,\bar{k}^2) - f(n,k^2)\right] + \frac{f(n,k^2)\, k^2}{\sqrt{k^4 + 4\bar{k}^2}} \right\}$$

$k_0^2 = 0$

$\longrightarrow$ EIGENFUNCTIONS :

$$e(n,\omega) = \frac{e(n,\omega^0)}{n - \left(1 + \frac{3\alpha_s}{\pi} K(\omega)\right)}$$

n_0 - POLE of $e(n,\omega)$ FOR $\omega = 0$

$$n_0 = 1 + 2.64\,\alpha_s$$

COLLINS
KWIECINSKI

$$G(x) \longrightarrow \sim \frac{1}{x^{n_0}}$$

ii) α_s running: $\quad \mathcal{L} = L_2$

$$L_2 \otimes f_n = L_1(\alpha_s \to \alpha_s(k^2),\ k_0^2 > 0) \otimes f_n$$

$$1 + \frac{3.6}{\pi}\alpha_s(k_0^2) \lesssim n_0 \lesssim 1 + 4\ln 2 \cdot \left(\frac{3}{\pi}\right)\alpha_s(k_0^2)$$

$$1.31 \lesssim n_0 \lesssim 1.72$$

in arb. dimensions: Ciafaloni et al., 1993

$$f_n(k,\mu^2,\varepsilon) = \delta^{(2+2\varepsilon)}(k) + \frac{\bar{\alpha}_s}{N-1}\int \frac{d^{2+2\varepsilon}q}{(2\pi\mu)^{2\varepsilon}}\frac{1}{\pi q^2}\cdot$$

$$\left\{ f_N(k-q,\mu^2,\varepsilon) - \frac{k\cdot(k-q)}{(k-q)^2} f_N(k,\mu^2,\varepsilon)\right\}$$

Hom. eq.: 2dim conformal invariant.

$$\curvearrowright \quad f_N \sim \left(\frac{k^2}{Q_0^2}\right)^{\gamma_N(\alpha_s)}$$

Eigenvalue equ.:

$$1 = \frac{\bar{\alpha}_s}{N-1}\left\{ 2\psi(1) - \psi(\gamma) - \psi(1-\gamma) + \mathcal{O}(\bar{\alpha}_s)\right\}$$

$$= \frac{\bar{\alpha}_s}{N-1}\left\{ \frac{1}{\gamma} + 2\sum_{n=1}^{\infty}\frac{\gamma^2}{n(n^2-\gamma^2)} + \mathcal{O}(\bar{\alpha}_s)\right\}$$

Solutions for i) $\frac{\bar{\alpha}_s}{N-1} \ll 1$ & ii) $\frac{\bar{\alpha}_s}{N-1} \gg 1$:

i) $$\gamma_N(\alpha_s) = \frac{\bar{\alpha}_s}{N-1} + 2\zeta(3)\left(\frac{\bar{\alpha}_s}{N-1}\right)^4 + 2\zeta(5)\left(\frac{\bar{\alpha}_s}{N-1}\right)^6 + \dots$$

ii) $$\gamma_N(\alpha_s) = \frac{1}{2} - \sqrt{\frac{N-N_\ell}{14\bar{\alpha}_s\zeta(3)}} + \dots$$

$$N_\ell = 1 + 4\alpha_s \ln 2$$

↑

branch point singularity.

KWIECINSKI

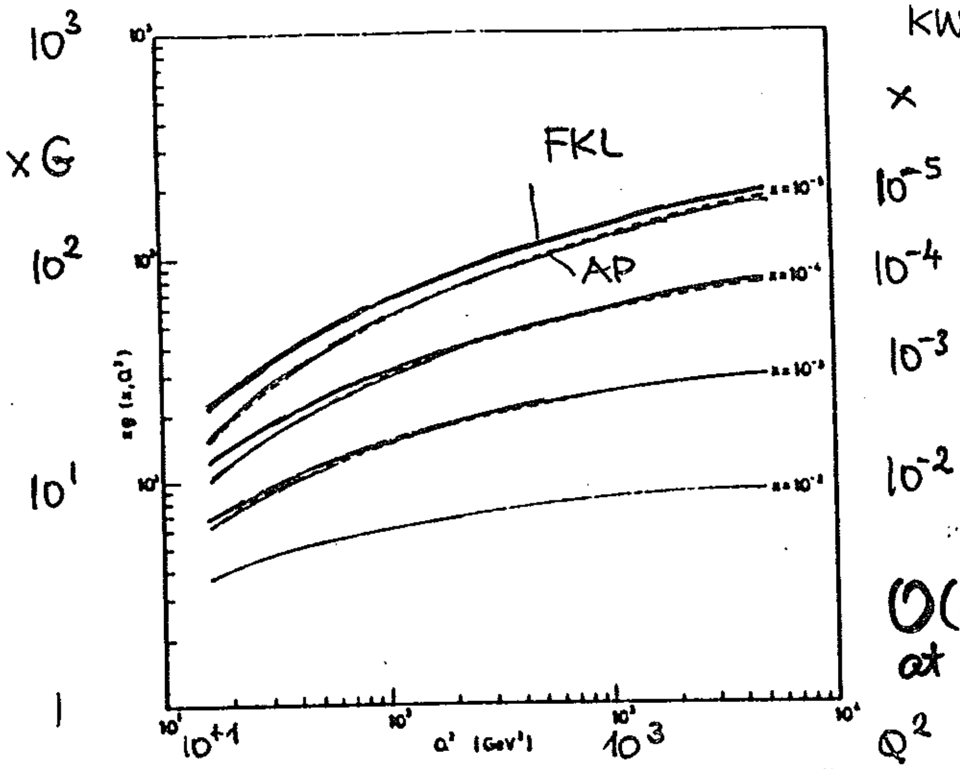

O(5%)
at HERA.

Fig. 3. The Q^2 evolution of gluon distributions beyond the leading ln $1/x$ approximation after corrections due to the constant term in the product $A_{gg}(\omega)\cdot A_{qg}(\omega)$ are included. The full line corresponds to the solution of the appropriately modified (3.6) and the dotted line to its leading log Q^2 counterpart

LEVIN
MARCHESINI
RYSKIN
WEBBER

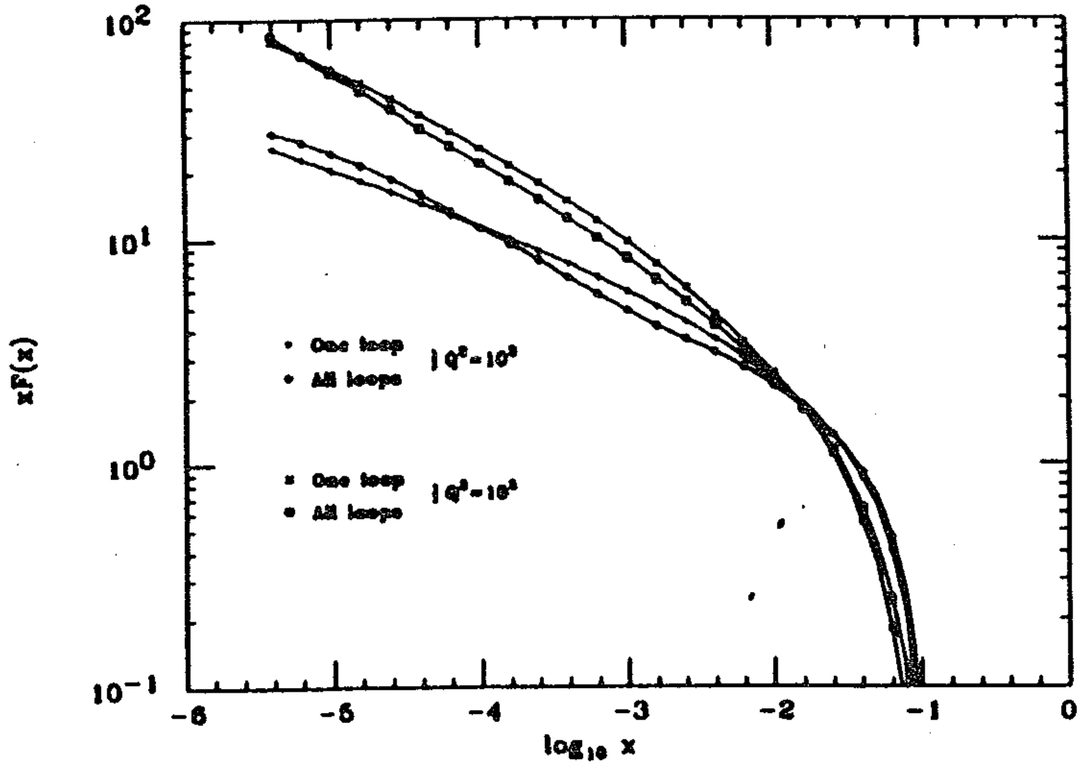

(MC)

Fig. 6. Monte Carlo structure functions for $Q_0 = 0.4$ GeV with starting condition $xF(x, Q_s^2) = \delta(x - 0.1)$ at $Q_s^2 = 5$ GeV^2.

LIPATOV eq. WITH RUNNING α_s :

- PUT IN BY HAND, 'INCORRECT' (KWIEC., COLLINS)

  $\rightarrow$ INCOMPLETE

- YIELDS A SIZEABLE INFRARED EFFECT, WHICH IS NOT UNDERSTOOD.

$\longrightarrow$ MARTIN et al. (AKMS)

$\Longrightarrow$
- FACTORIZATION WAS NOT PROVEN.
- CUT DEPENDENCE UNCLEAR.
- WHICH SCHEME ?

Fig.

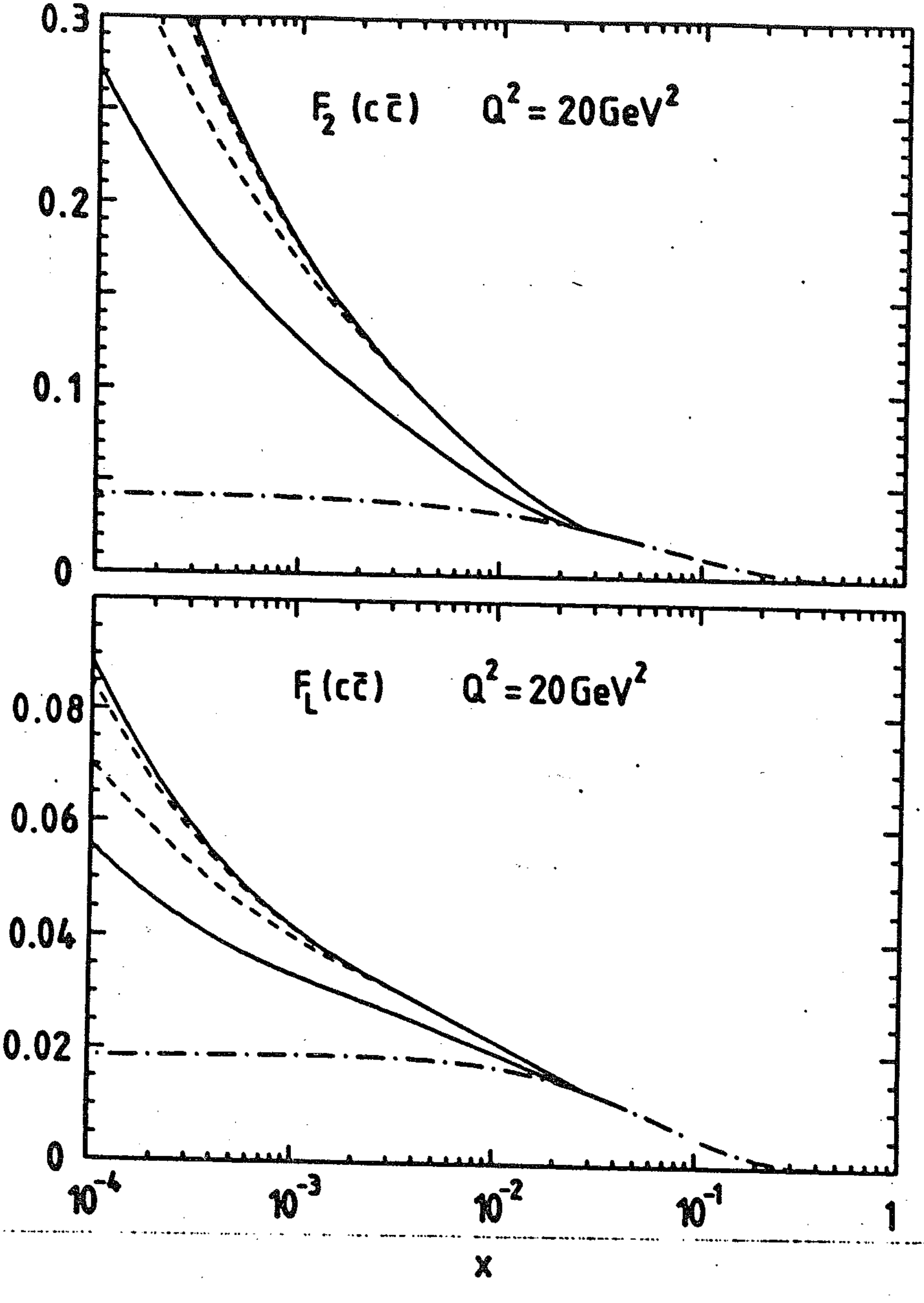

0.3
0.2
0.1
0
F2 (cc̄)
Q² = 20GeV²
0.08
0.06
0.04
0.02
0
FL (cc̄)
Q² = 20GeV²
10⁻⁴
10⁻³
10⁻²
10⁻¹
1
x

Fig. 7

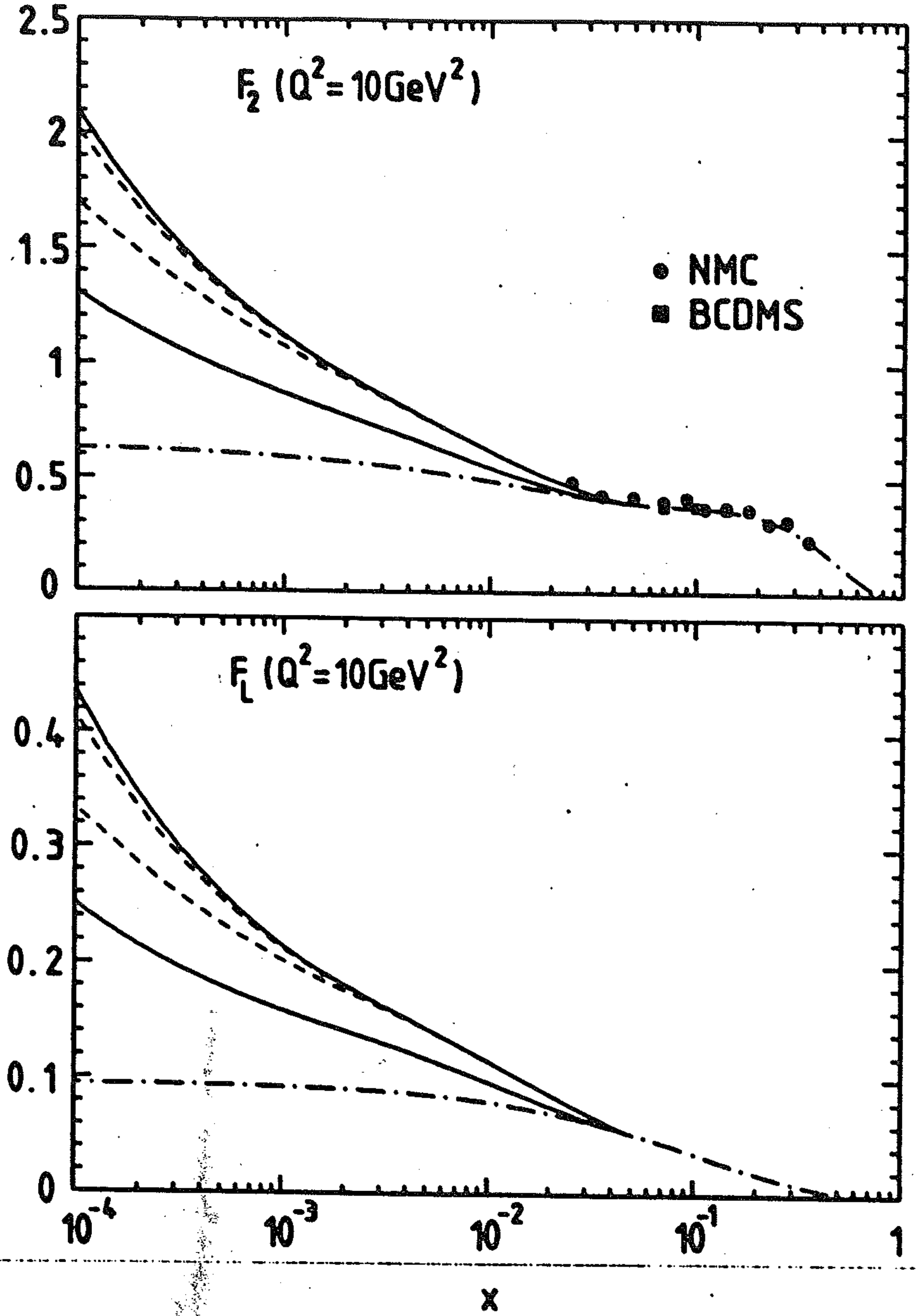

2.5
2
1.5
1
0.5
0
F_2 (Q^2= 10GeV^2)
NMC
BCDMS
F_L (Q^2=10GeV^2)
0.4
0.3
0.2
0.1
0
10^{-4}
10^{-3}
10^{-2}
10^{-1}
1
x

Fig. 5

b) THE ONSET OF SHADOWING AT SMALL X

– SCREENING : RESTORING UNITARITY
'PARTON RECOMBINATION'
GLR
& SUBSEQUENT WORK

⟹ QUANTIFICATION.

⟹ STRATEGY TO SEE THESE EFFECTS
IN $F_2^{em}(x, Q^2)$ $\Longleftrightarrow$ Λ, $xG(x, Q_0^2)$!

THE GLR EQUATION

a) TWIST-2 : EVOLUTION OF INDIVIDUAL PARTONS

$x \gtrsim 10^{-2}$ $\quad Q^2 > 10\ \mathrm{GeV}^2$

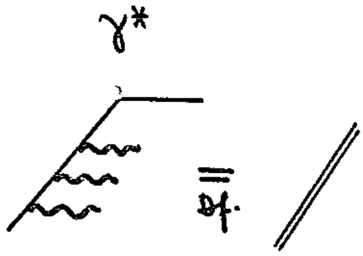

b) SEMI-HARD RANGE : x - GETTING SMALLER

$Q^2 \gtrsim 10 \ldots 50\ \mathrm{GeV}^2$

PARTONS RECOMBINE - FINITE 'PROTON' RADIUS

+ HIGH PARTONIC DENSITIES

DIAGRAMS:

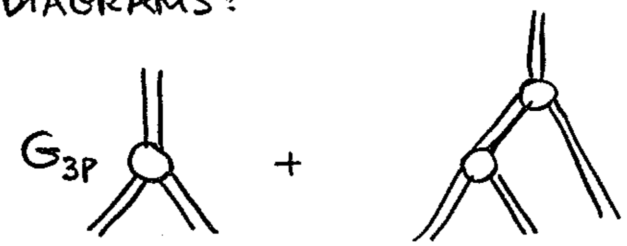

etc.

- GRIBOV, LEVIN, RYSKIN, 1982: LEADING PART AT EACH NODE
  $G + G \to G$ (Ladders)

- BARTELS 1992 (FURTHER CONTRIBUTIONS)

1^{st} FAN-DIAGRAM ~ 1% CORR.

MUELLER, QIU: DLA - EXPRESSION FOR G_{3P}.

$$G_{3P}(\xi) = \frac{3}{4}\pi^2 \frac{1}{\beta_0} e^{e^{\xi_0}} \exp\left[-(e^{\xi}+\xi)\right]$$

$$= \frac{3}{4}\pi^2 \frac{1}{\beta_0}\left(\frac{Q_0^2}{Q^2}\right)\frac{1}{\ln\left(\frac{Q^2}{\Lambda^2}\right)} \quad ; \text{HT}$$

$$= C \cdot \frac{\Lambda^2}{Q^2}$$

SUMMATION OF FAN DIAGRAMS:

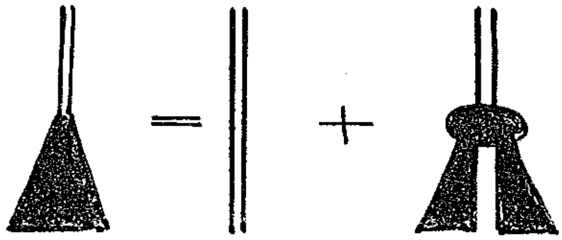

G_{3P}

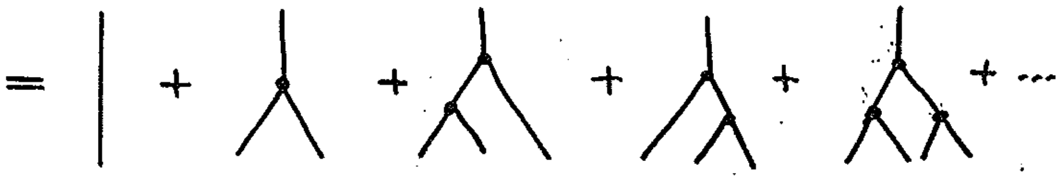

DLA

GLR: AGK CUTTING RULES (NOT YET FOUND IN QCD!

$$\frac{\partial^2 F(\xi,y)}{\partial\xi\,\partial y} = \underbrace{\frac{1}{2}}_{\text{DLA}} F(\xi,y) - C\exp\left[-(e^{\xi}+\xi)\right] F^2(\xi,y)$$

ASSUMPTION: $G_n(x_1,\dots,x_n) \simeq G(x_1)\dots G(x_n)$

IMPROVE WITH RESPECT TO REALISTIC INITIAL CONDITIONS:

(BARTELS, JB, SCHULER)

$$F(\xi,y) = G(\xi_0,y) + \int_{\xi_0}^{\xi} d\xi' \int_0^{y} dy' F(y',\xi')\left[\frac{1}{2} - C\exp\left[-(e^{\xi'}+\xi')\right] \times F(\xi',y')\right]$$

$\uparrow$

INPUT AT Q_0^2.

PROPERTIES OF THE EQUATION

i) SOLUTIONS ARE BOUNDED FROM ABOVE:

$F \leq F_0(\xi, y)$ (DLA) (AND BELOW $F_{Plup} \geq 0$!)

ii) $$\lim_{y \to \infty} F(y, \xi) = \frac{1}{2C} \exp\left[e^{\xi} + \xi\right] = \frac{1}{2C} \frac{Q^2}{\Lambda^2} \cdot \ln\left(\frac{Q^2}{\Lambda^2}\right) - \text{const}_{\xi \text{ or } Q^2}.$$

INDEPENDENT OF THE PARTICULAR CHOICE OF $G(y, \xi_0)$!

iii) $\exists!\ F(y, \xi)$

SOLUTION: QUADR. EQU. (LOCALLY) AT A SUFF. FINE GRID IN (ξ, y)

'VOLTERRA-TYPE' EQ. BOTH IN ξ & y.

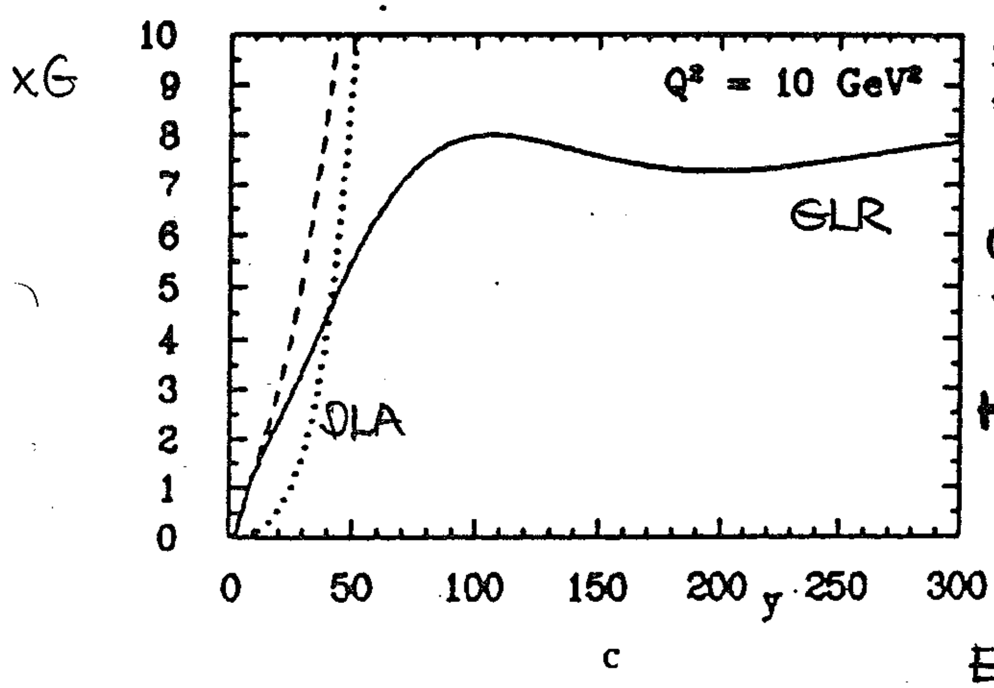

BARTELS, JB, SCHULER

OSCILLATIONS

'FEED BACK'

⟼ SATURATION

EXTREME y

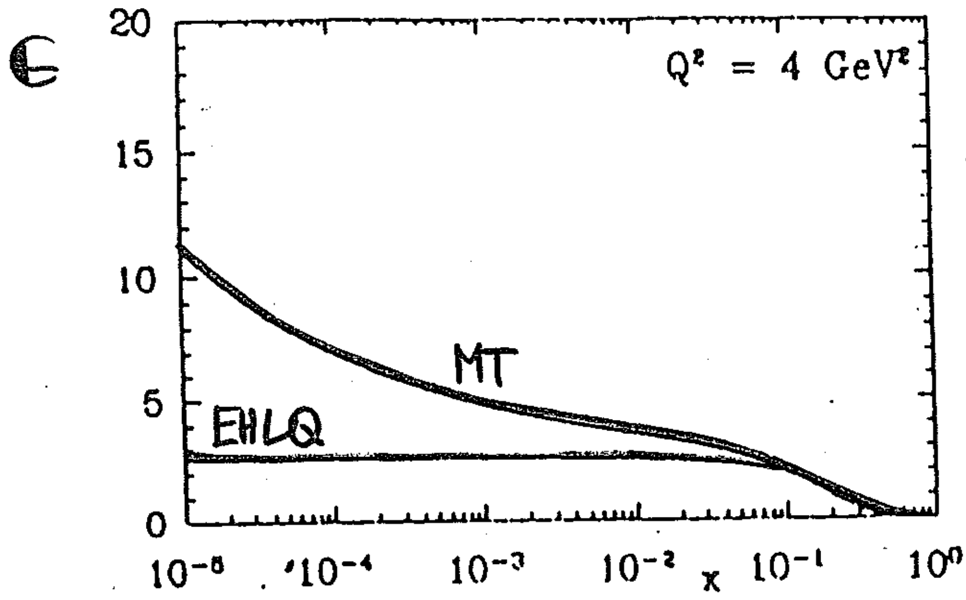

BARTELS, JB, SCHULER 1990

(cf. COLLINS, KWIECINSKI 1990; ALTMANN, GLÜCK, REYA, 1992 FOR SIMILAR INVESTIG.)

a

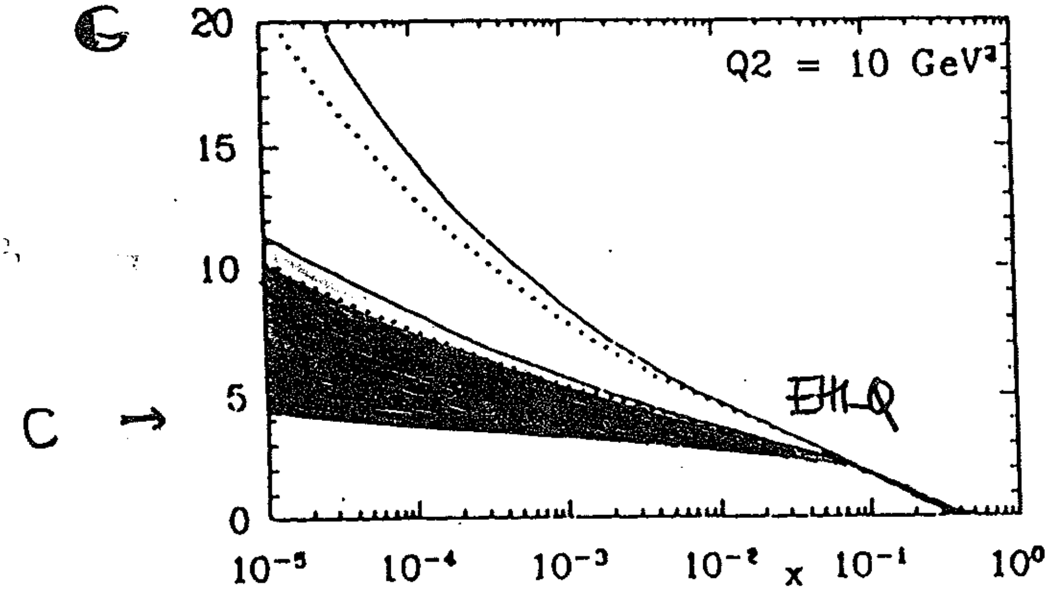

$C = C(\hat{Q}_0^2)$

$\hat{Q}_0 = \hat{Q}_0(R_{sc}$

b

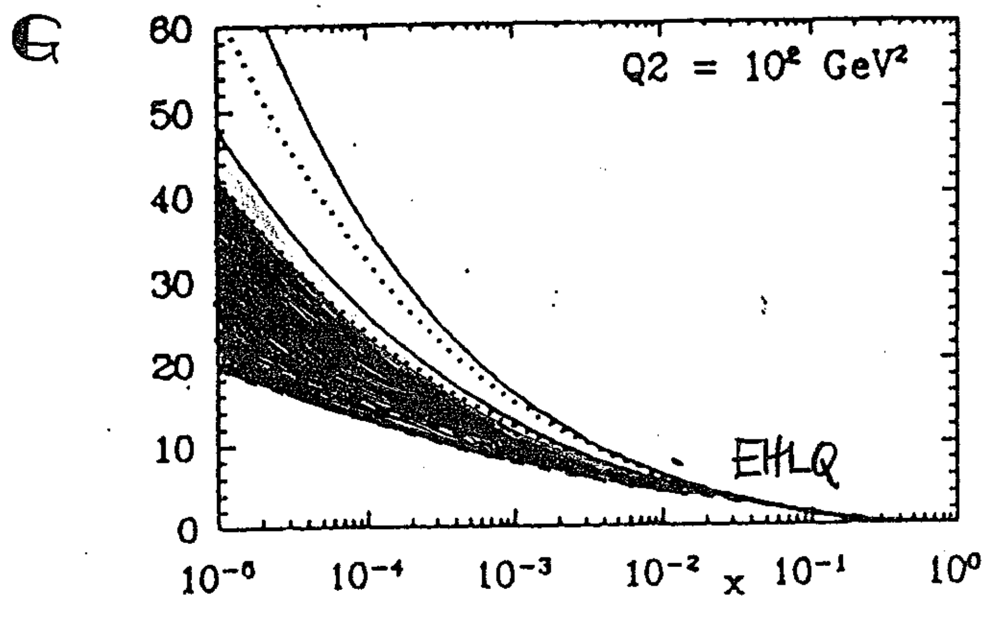

c

SEMICLASSICAL SOLUTIONS

BARTELS, JB, SCHULER ; COLLINS, KWIECINSKI

$$F(y,\xi) \underset{Df}{=} \exp(S(y,\xi))$$

$$S_{|y} S_{|\xi} = \frac{1}{2} - C \exp\left[S - e^{\xi} - \xi\right]$$

$$S_{|y} S_{|\xi} \gg S_{|y|\xi} \qquad (\xi \cdot y \gg 1)$$

$$\dot y = S_{|\xi}$$
$$\dot\xi = S_{|y}$$
$$\dot S = 2 S_{|y} S_{|\xi}$$
$$\dot S_{|\xi} = - C\exp\left(S - e^{\xi} - \xi\right) S_{|y}$$
$$\dot S_{|\xi} = -C\exp\left(S - e^{\xi} - \xi\right)\left(S_{|\xi} - 1 - e^{\xi}\right)$$

$C=0$ $\qquad \ddot y = \ddot \xi = 0$: STRAIGHT LINES IN ξ & y.

BARTELS, JB, SCHULER

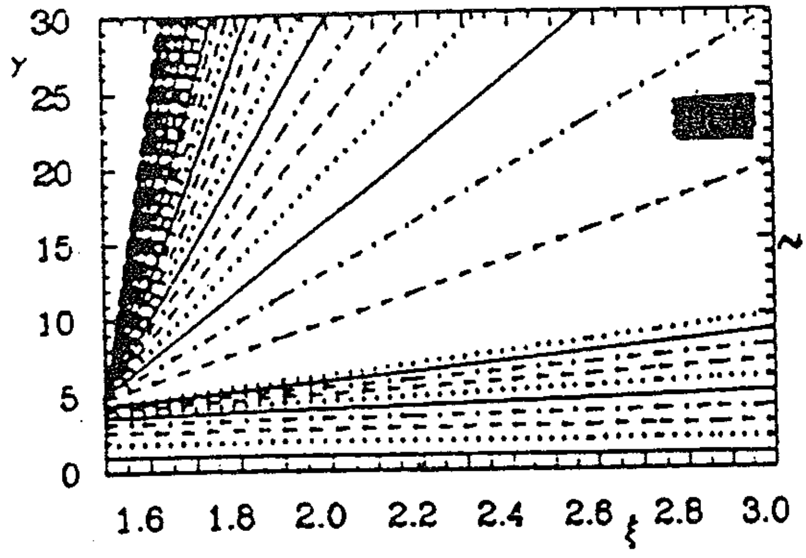

~AP

a

TRAJECTORIES STARTING BELOW

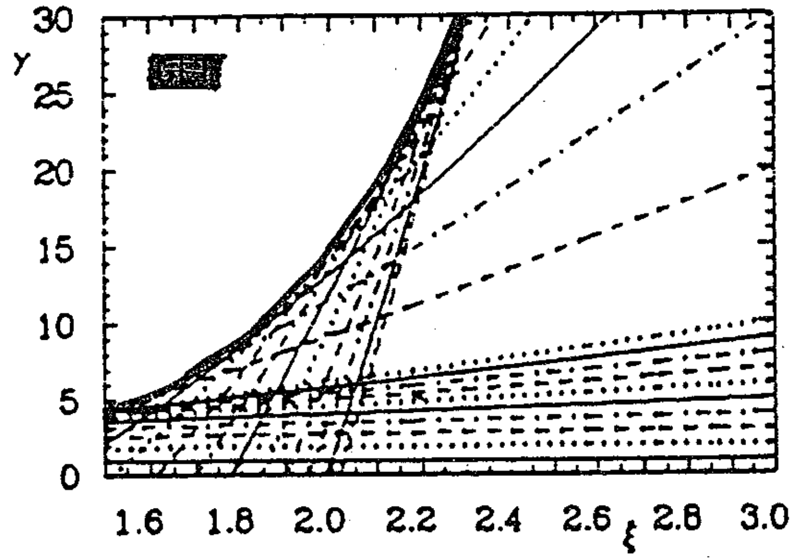

b

ABOVE THE 'CRITICAL' LINE

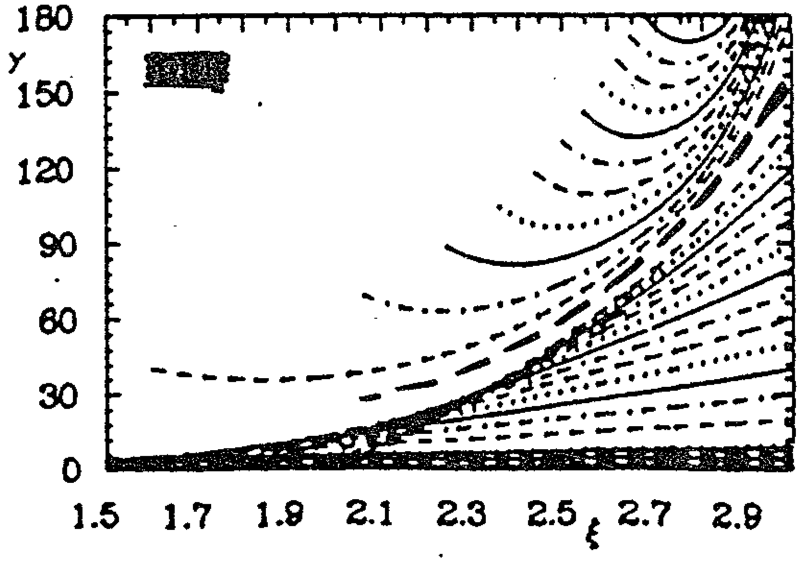

AP + FAN-DIAGRAMS (xG)

MUELLER, QIU

$$\frac{d\,x q_s(x,Q^2)}{d \ln Q^2} = \frac{\alpha_s}{2\pi}\left[P_{qg} \otimes xG \quad P_{qq} \otimes x q_s\right]$$

$$- \frac{27\,\alpha_s^2}{160\,R^2 Q^2}\left(x G(x,Q^2)\right)^2$$

$$+ \frac{\alpha_s}{\pi Q^2}\,\theta(x_0 - x)\int_x^{x_0} \frac{dx'}{x'}\,\gamma\left(\frac{x}{x'}\right) x G_H(x',Q^2)$$

$$\gamma(y) = -2y + 15y^2 - 30y^3 + 18y^4$$

$$\frac{d\,x G_H(x,Q^2)}{d \ln Q^2} = -\frac{81\,\alpha_s^2}{16\,R^2}\,\theta(x_0 - x)\int_x^{x_0} \frac{dx'}{x'}\left[x' G(x',Q^2)\right]^2$$

$$\frac{d\,x G(x,Q^2)}{d \ln Q^2} = \frac{\alpha_s}{2\pi}\left[P_{gg} \otimes xG + P_{gq} \otimes xq\right]$$

$$- \frac{81\,\alpha_s}{16\,R^2 Q^2}\,\theta(x_0 - x)\int_x^{x_0} \frac{dx'}{x'}\left[x' G(x',Q^2)\right]^2$$

USED IN: KMRS

$\longrightarrow$ MODIFICATIONS CURRENTLY WORKED OUT!

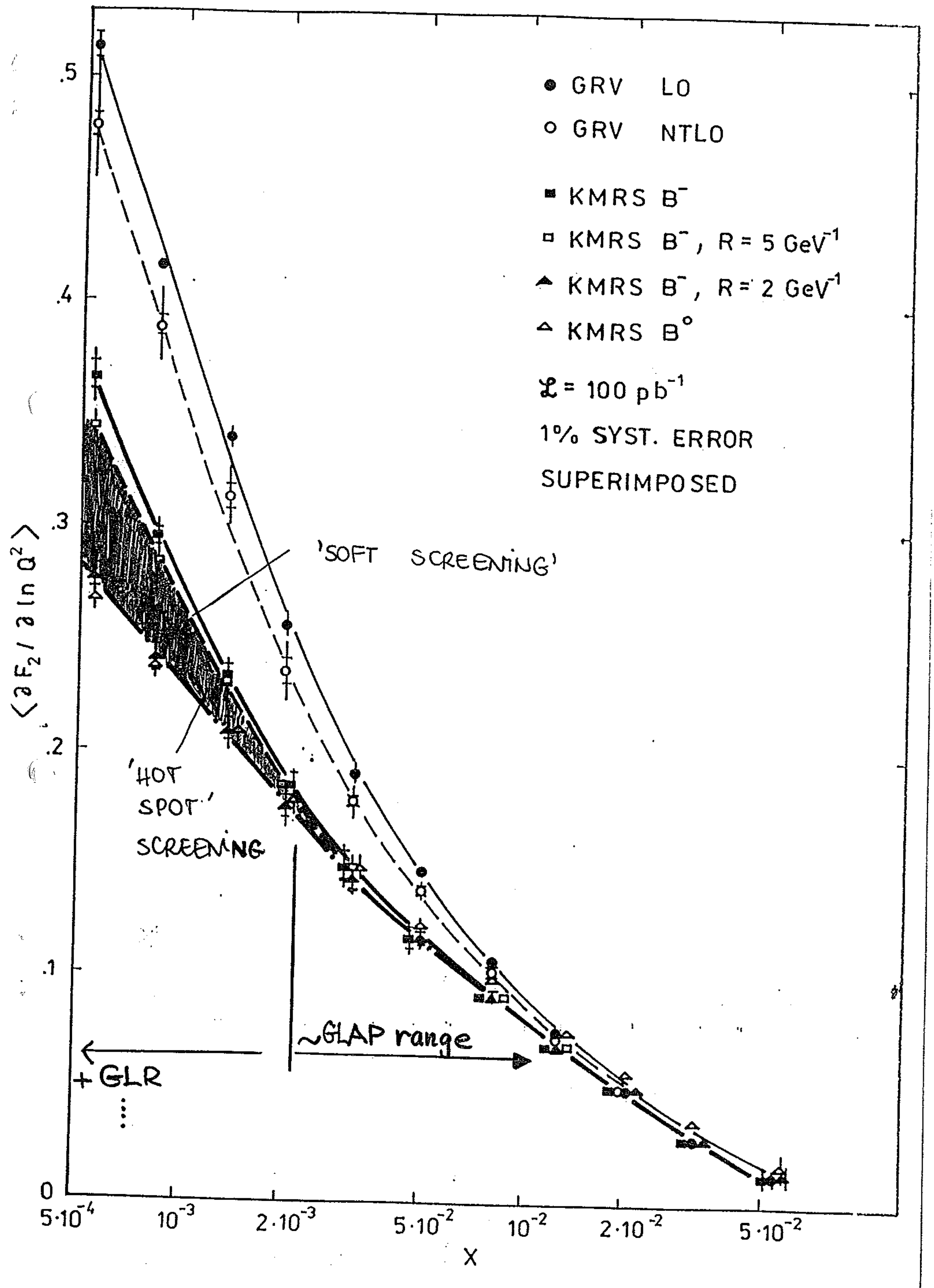
GRV LO
GRV NTLO
KMRS B⁻
KMRS B⁻, R = 5 GeV⁻¹
KMRS B⁻, R = 2 GeV⁻¹
KMRS B°
𝓛 = 100 pb⁻¹
1% SYST. ERROR
SUPERIMPOSED
'SOFT SCREENING'
'HOT SPOT' SCREENING
~GLAP range
+ GLR
⟨∂F₂ / ∂ ln Q²⟩
X
.5
.4
.3
.2
.1
0
5·10⁻⁴
10⁻³
2·10⁻³
5·10⁻²
10⁻²
2·10⁻²
5·10⁻²

CURRENT DEVELOPMENTS:

- LEVIN et al.
- BARTELS   corrections due to:

color neutral case.

$$\gamma_4 = \gamma_4^{GLR} \left(1 + \frac{1}{(N_c^2-1)^2} \cdot a\right)$$

Coefficient function(s) large ?! $\longrightarrow$ pole contribution.

PROBLEMS:

- 3 - ladder coupling in whole x range
- proof Θ - sign in QCD !
- screening for $x \to 0$?! / antiscreening for larger x
- WHERE IS THE TURNING POINT $x_0 = x_0(Q^2)$! ?

$\longrightarrow$ requieres full calculation (six point function in center).

c) $\boxed{k_\perp \text{ FACTORIZATION } \& \ F_L\,,\, F_2}$

1 Motivation

- TRADITIONAL APPROACH: GLAP

COEFFICIENT & SPLITTING FUNCTIONS ARE ONLY X DEPENDENT.

$$\langle k_\perp^2 \rangle / Q^2 \ll 1$$

- $\longrightarrow$ related to strong $k_\perp$ ordering

- SMALL X: IMPORTANT TERMS FROM OTHER SITUATIONS $\longrightarrow$ LIPATOV EQUATION.

- F_2, F_L – TO BE CALCULATED IN THE 'NON-COLLINEAR' PICTURE, I.E. ALLOWING FOR GLUON MOMENTA

$$k_\mu = \xi q'_\mu + \eta P_\mu + k_{\perp\mu}$$

HIGH ENERGY LIMIT : LEVIN, RYSKIN 1991

PROBLEMS TO BE SOLVED:

1) FACTORIZATION OF THE INCOMING PARTON DENSITY

2) $\boxed{\text{CONVOLUTION}}$ IN X-SPACE

$$F(x) = \int_0^1 dx_1 \int_0^1 dx_2 \, \delta(x - x_1 x_2) \, f(x_1) \, D(x_2)$$

f AT $x_1 \sim 1$ SAMPLES D AT $x_2 \sim x$ AND VICE VERSA!

$\longrightarrow$ TO KNOW f AT $x_1 \approx x$ IS NOT ENOUGH!

$\longmapsto$ EXPL.

3) HOW TO MAKE CONTACT WITH THE REAL GLUON & QUARK DENSITIES?

$\longrightarrow$ SCHEME DEPENDENCE

$\longrightarrow$ TREATMENT OF THE COLLINEAR SINGULARITIES

$\longrightarrow$ THIS OPENS THE WAY TO MORE GENERAL GLUON DENSITIES; ONE HAS NOT TO RELY ON THE $\alpha_s = \text{CONST.}$ LIPATOV SOLUTION etc.

4) TECHNICAL QUESTION: LOOK FOR A SUITABLE REF. FRAME; $\longleftrightarrow$ CCH.

3 $\quad k_\perp$ Factorization in the DIS Scheme

- The $k_\perp$ integration starts at $K^2 = 0$.
  However, a physical definition of $\partial x G(x, K^2)/\partial K^2$ is only possible for $K^2 \gtrsim Q_0^2$!

$\Longrightarrow$ Naive $k_\perp$ Factorization fails.

Consider:

$$Q_0^2 \ll Q^2$$

$$\text{For } K^2 \leq Q_0^2\text{: } f_i^{\gamma G}\left(\frac{K^2}{Q^2}, \frac{x}{\eta}\right) \Longrightarrow f_i^{\gamma G}\left(\frac{K^2}{Q^2} \to 0, \frac{x}{\eta}\right), \; i = 2, L$$

- The 'naive' factorization relation:

$$F_i(x, Q^2) = \int_0^1 \int_0^1 dx_1 dx_2 \delta(x - x_1 x_2) \int \frac{d^2_{\perp} k}{\pi} f_i(x_1, K^2/Q^2) \frac{\partial x_2 G(x_2, K^2)}{\partial K^2}$$

has to be replaced by:

$$\boxed{\begin{aligned} F_L(x, Q^2) &= \int_x^1 \frac{d\eta}{\eta} f_L\left(\frac{x}{\eta}\right) \eta G(\eta, Q_0^2) + \int_x^1 \frac{d\eta}{\eta} \int_{Q_0^2}^{K^2_{max}} dK^2 f_L\left(\frac{x}{\eta}, \frac{K^2}{Q^2}\right) \frac{\partial \eta G(\eta, K^2)}{\partial K^2} \\ F_2(x, Q^2) &= F_2^{coll}(x, Q^2) \\ &+ \int_x^1 \frac{d\eta}{\eta} \int_{Q_0^2}^{K^2_{max}} dK^2 \left\{ f_2\left(\frac{x}{\eta}, \frac{K^2}{Q^2}\right) - f_2\left(\frac{x}{\eta}, \frac{\Lambda^2}{Q^2}\right) \theta(Q^2 - K^2) \right\} \frac{\partial \eta G(\eta, K^2)}{\partial K^2} \end{aligned}}$$

$F_2^{coll}(x, Q^2)$ denotes the structure function F_2 calculated for collinear initial state gluons in the DIS scheme.

$$\sum_\lambda \epsilon^*_\mu(\lambda) \epsilon_\nu(\lambda) = \frac{P_\mu P_\nu}{k^2}$$

The scale of α_s:

For the present leading order calculation one has to choose a typical hard scale, characterizing the process: Q^2, W^2.

4 The Structure Functions

$$\frac{d^2\sigma}{dQ^2dy} = 2\pi\alpha^2\frac{Ms}{(s-M^2)^2}\frac{1}{Q^4}L_{\mu\nu}W^{\mu\nu}$$

$$L_{\mu\nu} = 2\left[l_\mu l'_\nu + l'_\mu l_\nu - g_{\mu\nu}l.l'\right]$$

$$W_{\mu\nu} = \frac{1}{4\pi}\sum_n \langle P|J_\mu^{em\dagger}(0)|n\rangle\langle n|J_\nu^{em}(0)|P\rangle(2\pi)^4\delta^{(4)}(P+q-p_n)$$

$$W_{\mu\nu} = \left(-g_{\mu\nu} + \frac{q_\mu q_\nu}{q^2}\right)W_1(x,Q^2) + \frac{1}{M^2}\left[\left(P_\mu - \frac{P.q}{q^2}q_\mu\right)\left(P_\nu - \frac{P.q}{q^2}q_\nu\right)\right]W_2(x,Q^2)$$

$$F_2(x,Q^2) = xT^1_{\mu\nu}W^{\mu\nu} = x\left(-g_{\mu\nu} + \frac{12x^2}{Q^2}P_\mu P_\nu\right)W^{\mu\nu}$$
$$F_L(x,Q^2) = xT^2_{\mu\nu}W^{\mu\nu} = \frac{8x^3}{Q^2}P_\mu P_\nu W^{\mu\nu}$$

The projections onto $-g_{\mu\nu}$ and $P_\mu P_\nu$ are

$$-g^{\mu\nu}\widehat{W}_{\mu\nu} = 32\pi\alpha_s e_q^2\left\{\frac{(p_1.P)^2+(p_2.P)^2}{\hat{t}\hat{u}} - \frac{Q^2}{K^2}\left[\frac{p_1.P}{\hat{t}} - \frac{p_2.P}{\hat{u}}\right]^2\right\}$$
$$P^\mu P^\nu\widehat{W}_{\mu\nu} = 64\pi\alpha_s e_q^2\frac{1}{K^2}\left\{-2\frac{(p_1.P)^2(p_2.P)^2}{\hat{t}\hat{u}} + \frac{(p_1.P)^3(p_2.P)}{\hat{t}^2} + \frac{(p_1.P)(p_2.P)^3}{\hat{u}^2}\right\}$$

$\longleftrightarrow$ CIAFALONI et al

$K_\perp^2 \to 0$

$$-g^{\mu\nu}\widehat{W}_{\mu\nu} = 8\pi\alpha_s e_q^2\left\{\frac{\hat{t}}{\hat{u}} + \frac{\hat{u}}{\hat{t}} - 2\frac{\hat{s}Q^2}{\hat{t}\hat{u}}\right\}$$
$$P_\mu P_\nu\widehat{W}_{\mu\nu} = 8\pi\alpha_s e_q^2\hat{s}$$

GLAP – coeff. functions.

$+ \ 2^{\text{dim}}$ PS.

$$\boxed{F_L\,(x, Q^2)}$$

$$f_L^{gG}(K^2,x,Q^2) = -\frac{1}{4\pi}\int dPS^{(2)} x T^2_{\mu\nu}\widehat{W}^{\mu\nu}$$
$$= \frac{\alpha_s e_q^2}{4\pi}\left\{\frac{4Q^4}{K^4 x}G_{1L}(\beta,\zeta) + \frac{xQ^2}{K^2}\frac{1}{\sqrt{1-\zeta}}\log\left|\frac{1+\sqrt{1-\zeta}}{1-\sqrt{1-\zeta}}\right|G_{2L}(\beta,\zeta)\right.$$
$$\left. + \frac{2xQ^2}{K^2}G_{3L}(\beta,\zeta)\right\}$$

with

$$\zeta = \frac{4K^2x^2}{Q^2}$$

and

$$G_{iL}(\beta,\zeta) = -\sum_{j=0}^{4} g_{ji}^{L}(\beta)\left(\frac{\zeta}{W(\zeta)}\right)^j$$

where

$$W(\zeta) = 1-\zeta+\sqrt{1-\zeta} \qquad \rightarrow \text{TAB.}$$

$\lim_{k^2\to 0}$:

$$\underline{f_L^{gG(0)}(x,Q^2) = \frac{8x^3}{Q^2}\frac{1}{4\pi}\int dPS^{(2,0)}P_\mu P_\nu \widehat{W}^{\mu\nu} = \frac{2}{\pi}e_q^2\alpha_s x^2(1-x)}$$

$$F_L(x,Q^2) = \int_x^1 \frac{d\eta}{\eta}\, f_L\left(\frac{x}{\eta}\right)\eta\, G(\eta,Q_0^2)$$
$$+ \int_x^1 \frac{d\eta}{\eta}\int_{Q_0}^{K^2_{max}} dk^2\, f_L\left(\frac{x}{\eta},\frac{k^2}{Q^2}\right)\frac{\partial \eta\, G(\eta,k^2)}{\partial k^2}$$

$$
\begin{aligned}
g_{01}^{(L)}(\beta) &= -\frac{1}{8}+\frac{1}{4}\cos\beta-\frac{1}{4}\cos^3\beta+\frac{1}{8}\cos^4\beta \\
g_{02}^{(L)}(\beta) &= -\frac{1}{4}+2\cos\beta-\cos^2\beta-3\cos^3\beta+\frac{9}{4}\cos^4\beta \\
g_{03}^{(L)}(\beta) &= -\frac{1}{4}+6\cos\beta-\frac{9}{2}\cos^2\beta-10\cos^3\beta+\frac{35}{4}\cos^4\beta \\
g_{11}^{(L)}(\beta) &= \cos\beta-\frac{3}{4}\cos^2\beta-\frac{3}{2}\cos^3\beta+\frac{5}{4}\cos^4\beta \\
g_{12}^{(L)}(\beta) &= \frac{1}{4}+\frac{13}{2}\cos\beta-\frac{15}{2}\cos^2\beta-\frac{21}{2}\cos^3\beta+\frac{45}{4}\cos^4\beta \\
g_{13}^{(L)}(\beta) &= 1+18\cos\beta-24\cos^2\beta-30\cos^3\beta+35\cos^4\beta \\
g_{21}^{(L)}(\beta) &= \frac{3}{16}+\frac{9}{8}\cos\beta-\frac{9}{4}\cos^2\beta-\frac{15}{8}\cos^3\beta+\frac{45}{16}\cos^4\beta \\
g_{22}^{(L)}(\beta) &= \frac{5}{4}+\frac{27}{4}\cos\beta-15\cos^2\beta-\frac{45}{4}\cos^3\beta+\frac{75}{4}\cos^4\beta \\
g_{23}^{(L)}(\beta) &= \frac{7}{2}+18\cos\beta-42\cos^2\beta-30\cos^3\beta+\frac{105}{2}\cos^4\beta \\
g_{31}^{(L)}(\beta) &= \frac{3}{16}+\frac{6}{16}\cos\beta-\frac{15}{8}\cos^2\beta-\frac{5}{2}\cos^3\beta+\frac{35}{4}\cos^4\beta \\
g_{32}^{(L)}(\beta) &= \frac{9}{8}+\frac{9}{4}\cos\beta-\frac{45}{4}\cos^2\beta-\frac{15}{4}\cos^3\beta+\frac{105}{8}\cos^4\beta \\
g_{33}^{(L)}(\beta) &= 3+6\cos\beta-30\cos^2\beta-10\cos^3\beta+35\cos^4\beta \\
g_{41}^{(L)}(\beta) &= \frac{3}{64}-\frac{15}{32}\cos^2\beta+\frac{35}{64}\cos^4\beta \\
g_{42}^{(L)}(\beta) &= \frac{9}{32}-\frac{45}{16}\cos^2\beta+\frac{105}{32}\cos^4\beta \\
g_{43}^{(L)}(\beta) &= \frac{3}{4}-\frac{15}{2}\cos^2\beta+\frac{35}{4}\cos^4\beta
\end{aligned}
$$

4. STRUCTURE FUNCTIONS AT HERA

- HOW TO GET THEM
- PARTONDISTRIBUTIONS
- Λ_{QCD}, α_s ... PROSPECTS.

WAYS TO EXTRACT STRUCTURE FUNCTIONS

CHARGED LEPTON – N DIS

NC

$$\sigma^{\pm}_{NC} = \frac{d\sigma^{\pm}_{NC}}{dx\,dQ^2} \quad , \quad \sigma^{\pm}_{CC} = \frac{d\sigma^{\pm}_{CC}}{dx\,dQ^2}$$

$F_2(x,Q^2)$:

$$\sigma^{\pm}_{NC} \quad (K_Z(Q^2) \ll 1)$$

i.e. $\frac{Q^2}{Q^2+M_Z^2} \ll 1 \quad , \quad Q^2 \ll M_Z^2$

$(Q^2 \lesssim 700\ \text{GeV}^2)$.

$$\boxed{F_2(x,Q^2) = \frac{x\,Q^4}{2\pi\alpha^2}\,\frac{1}{Y_+}\cdot\sigma^{\pm}_{NC}(x,Q^2)}$$

APPROACHING EVEN HIGHER Q^2:

$$\mathbb{B}_+(\lambda) = \frac{1}{2}\left[\sigma^{+}_{NC}(\lambda) + \sigma^{-}_{NC}(-\lambda)\right]\frac{1}{Y_+} = F_2 + \overbrace{(-v+\lambda a)}^{=0;\ v/a=\lambda\approx 0.} G_2 K_Z$$

$$+ (v^2 + a^2 - 2va\lambda)\, H_2 K_Z^2$$

$\uparrow$

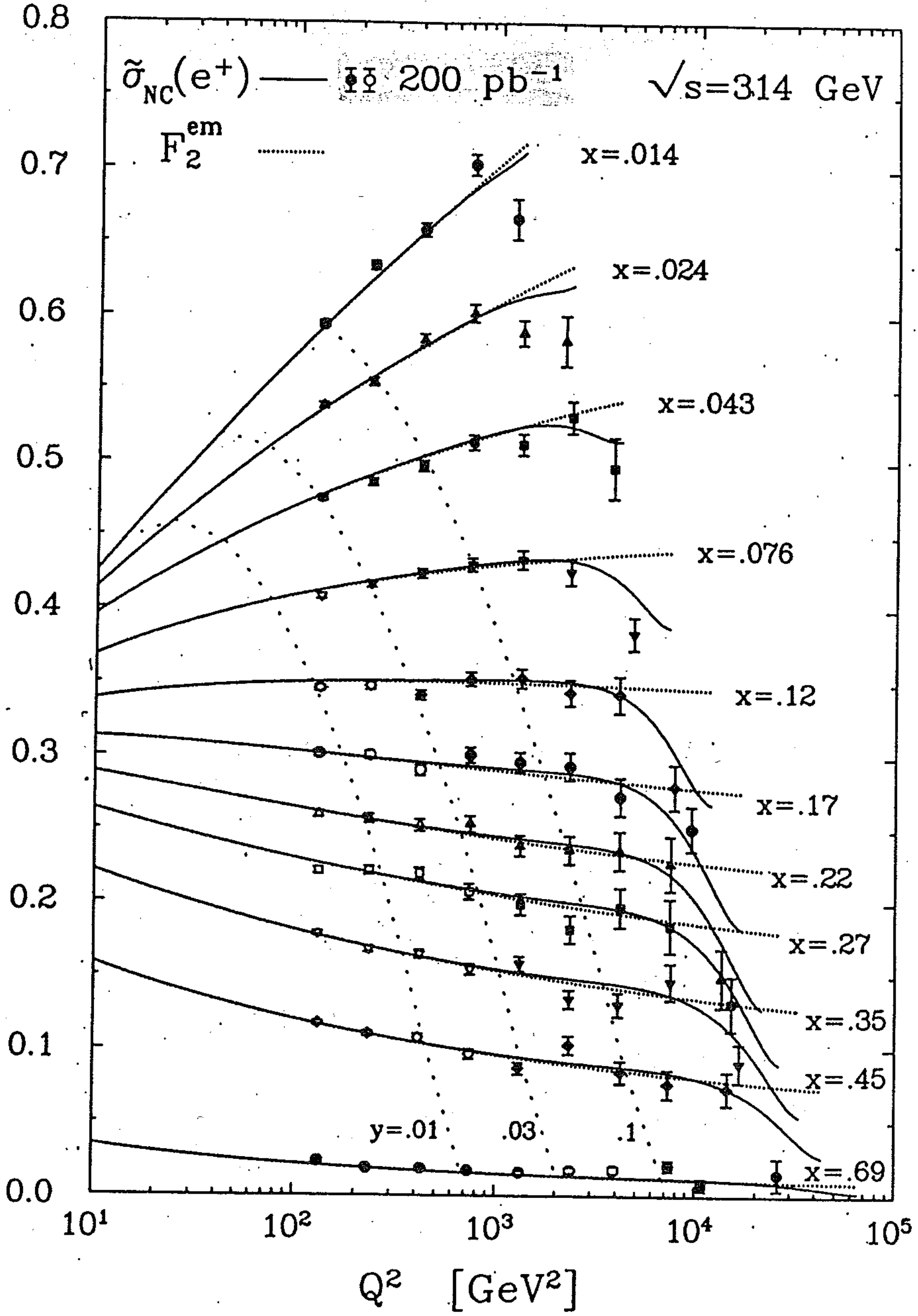

$\tilde{\sigma}_{NC}(e^+)$
200 pb^{-1}
$\sqrt{s}$=314 GeV
F_2^{em}
x=.014
x=.024
x=.043
x=.076
x=.12
x=.17
x=.22
x=.27
x=.35
x=.45
x=.69
y=.01
.03
.1
0.8
0.7
0.6
0.5
0.4
0.3
0.2
0.1
0.0
10^1
10^2
10^3
10^4
10^5
Q^2 [GeV^2]

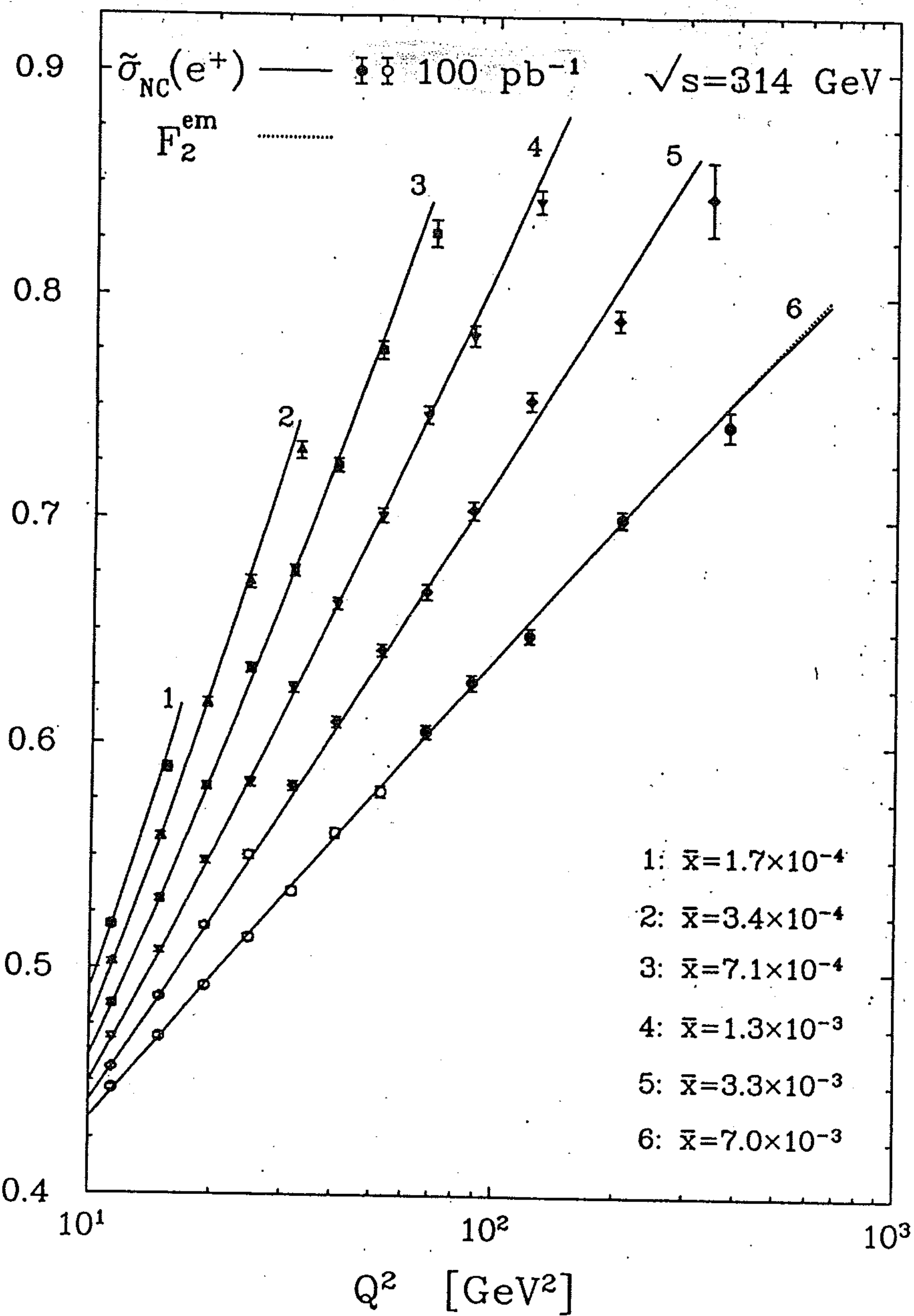
$\tilde{\sigma}_{NC}(e^+)$
100 pb^{-1}
$\sqrt{s}$=314 GeV
F_2^{em}
1
2
3
4
5
6
1: $\bar{x}=1.7\times10^{-4}$
2: $\bar{x}=3.4\times10^{-4}$
3: $\bar{x}=7.1\times10^{-4}$
4: $\bar{x}=1.3\times10^{-3}$
5: $\bar{x}=3.3\times10^{-3}$
6: $\bar{x}=7.0\times10^{-3}$
0.4
0.5
0.6
0.7
0.8
0.9
10^1
10^2
10^3
Q^2 [GeV^2]

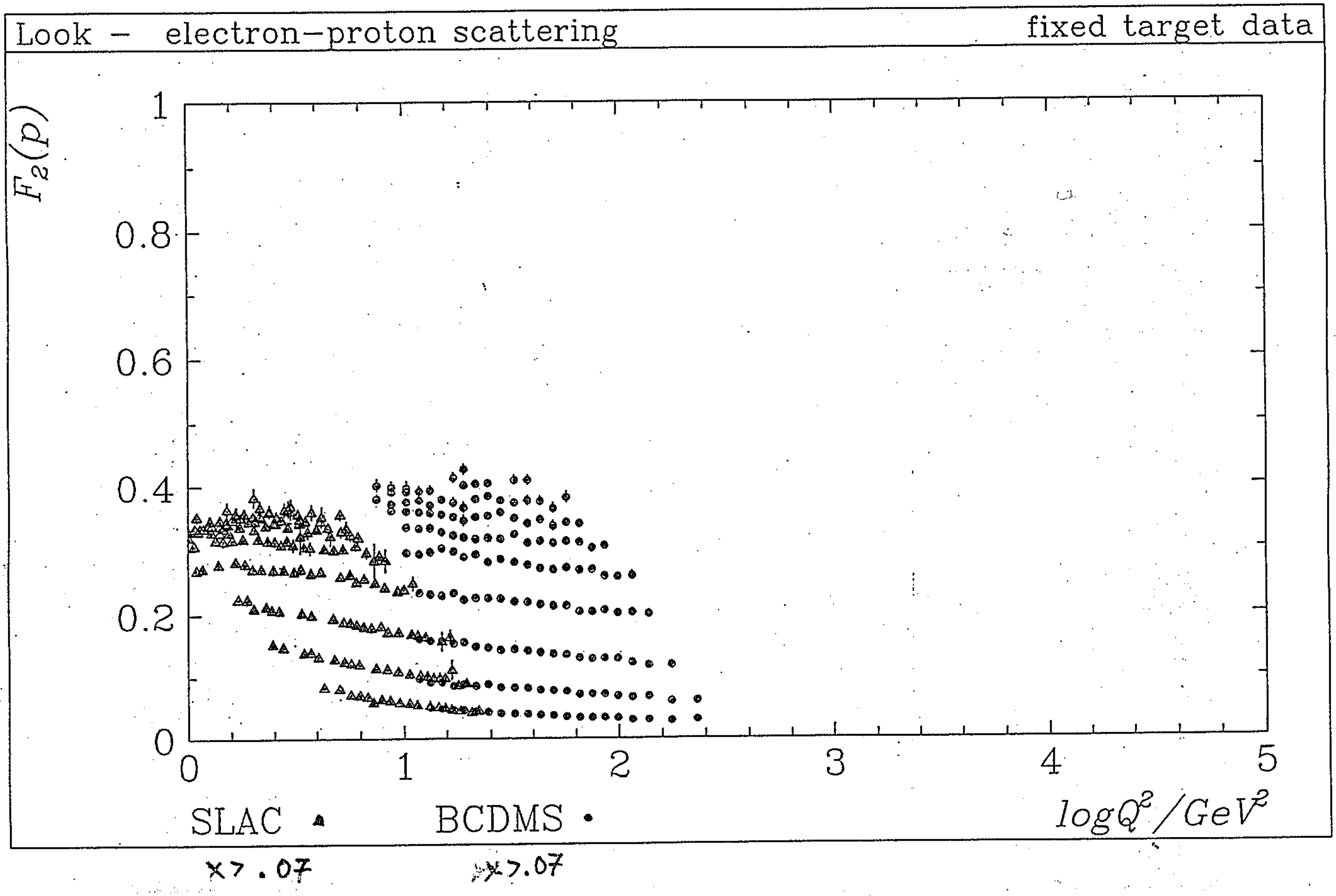

Look - electron-proton scattering
fixed target data
$F_2(p)$
1
0.8
0.6
0.4
0.2
0
0
1
2
3
4
5
SLAC
BCDMS
$log Q^2 / GeV^2$
x > .07
x > .07

BLUMLEIN, KLEIN

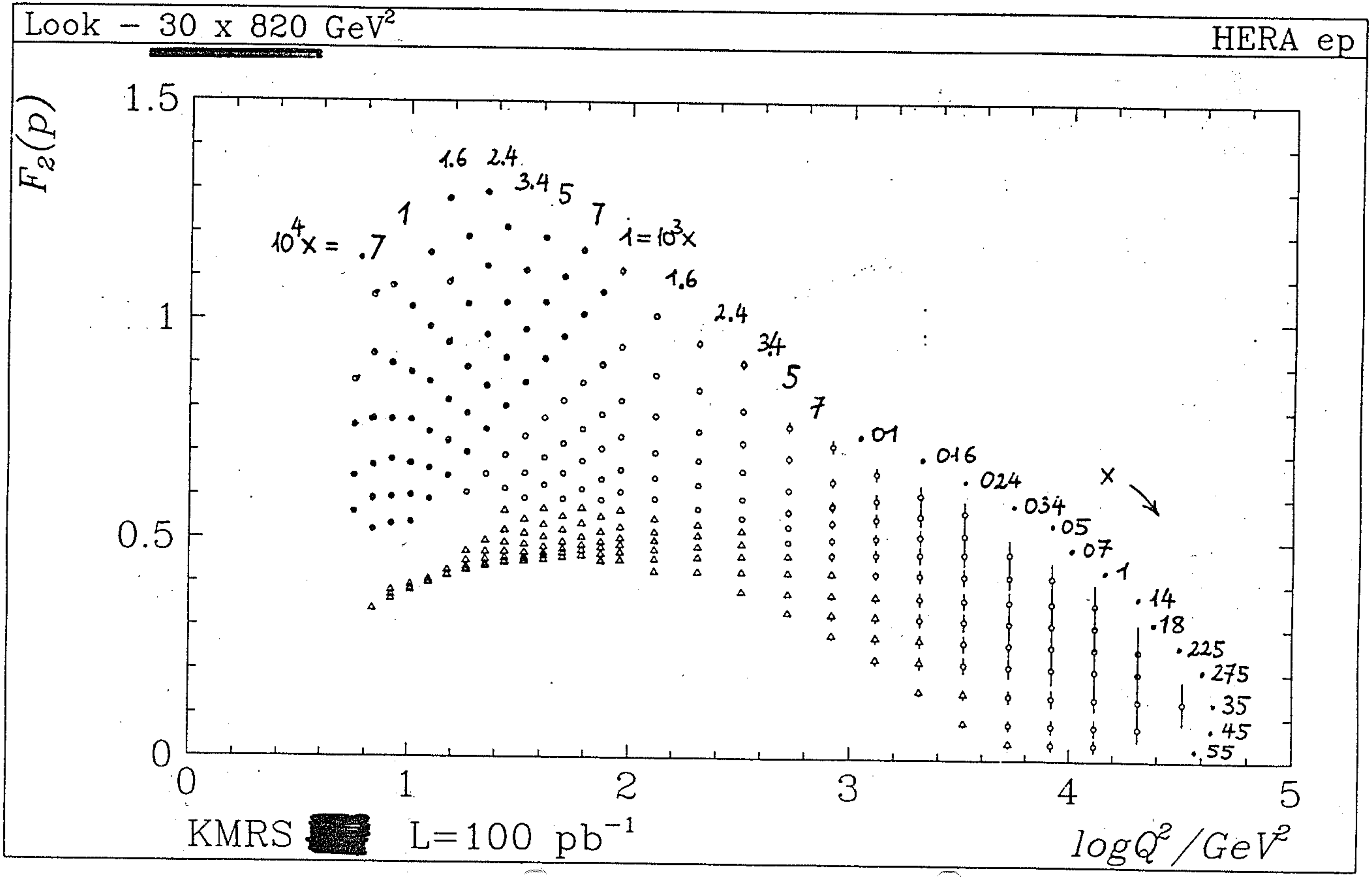

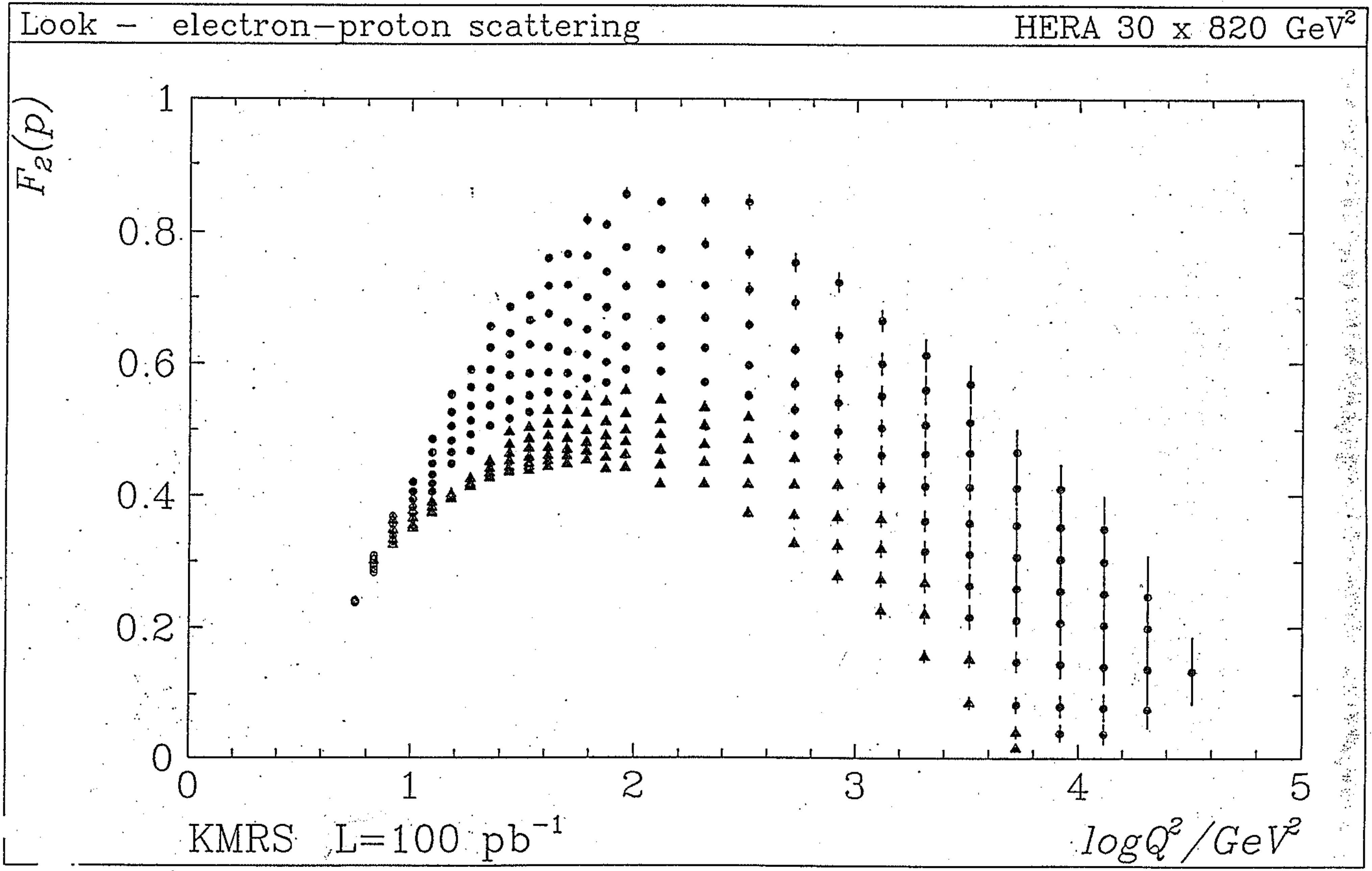
Look – electron–proton scattering
HERA 30 x 820 GeV^2
$F_2(p)$
1
0.8
0.6
0.4
0.2
0
0
1
2
3
4
5
KMRS L=100 pb^{-1}
$logQ^2/GeV^2$

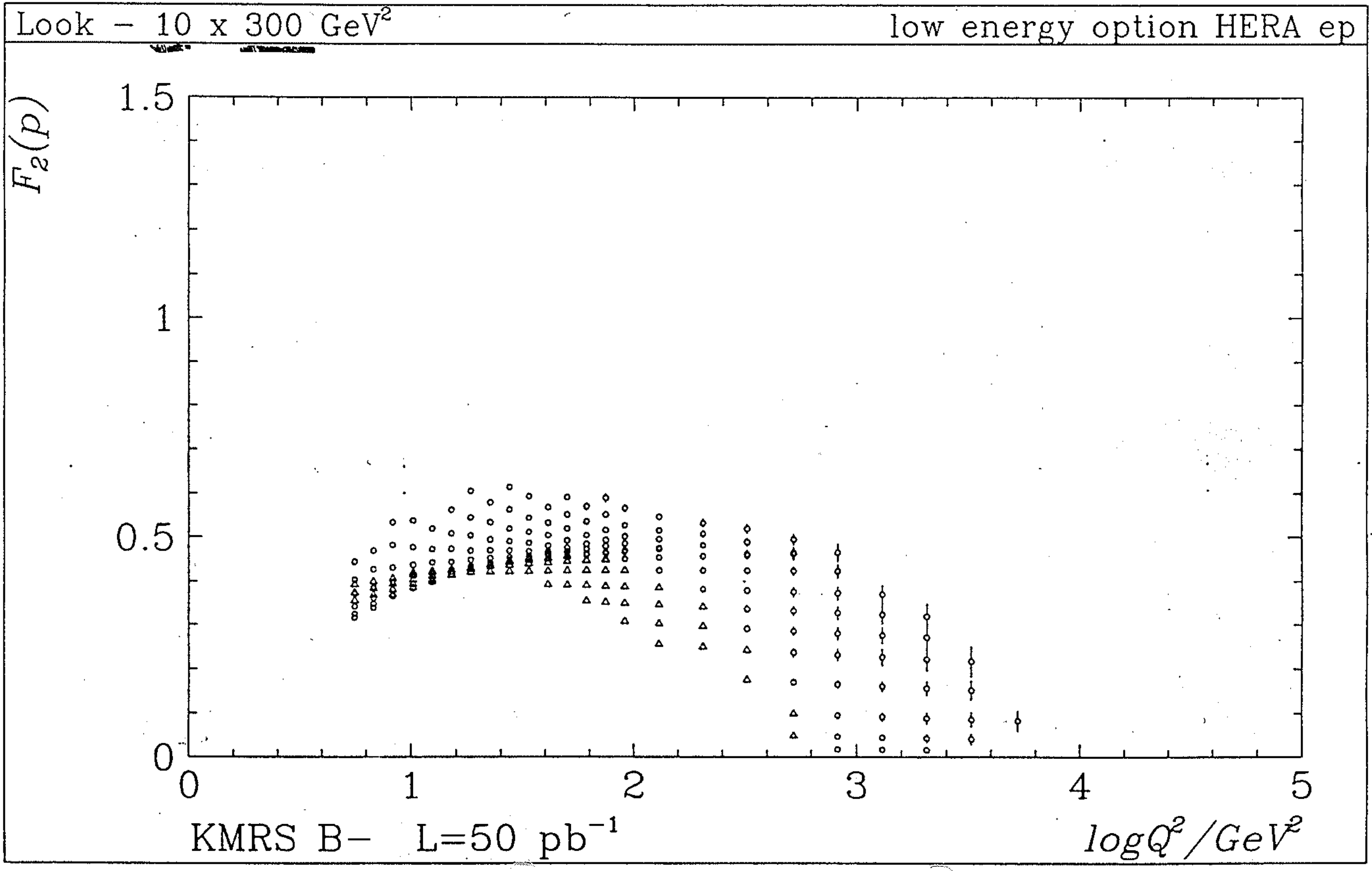
Look - 10 x 300 GeV^2
low energy option HERA ep
$F_2(p)$
1.5
1
0.5
0
0
1
2
3
4
5
KMRS B- L=50 pb^{-1}
$logQ^2/GeV^2$

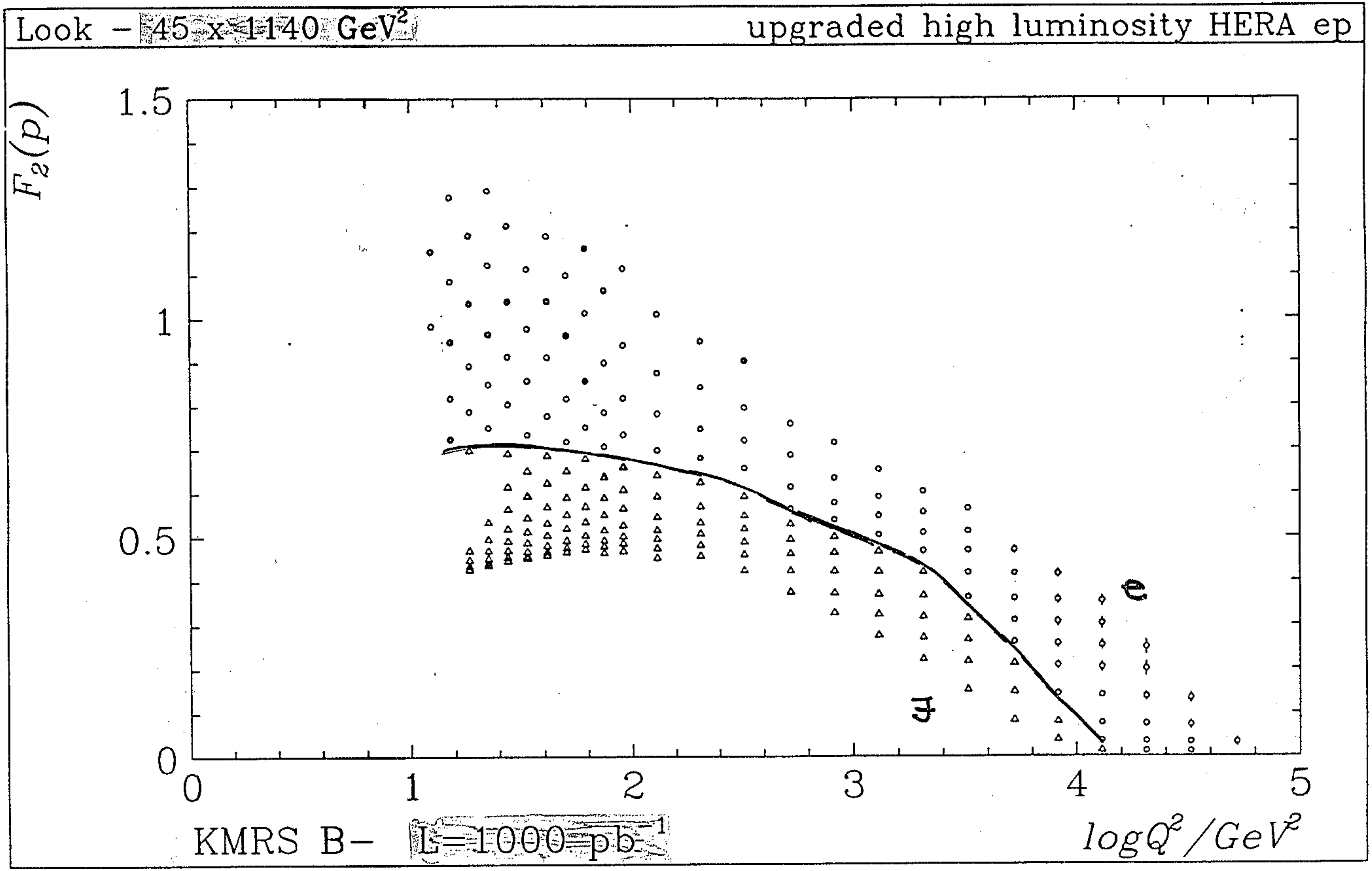

Look - 45 x 1140 GeV^2
upgraded high luminosity HERA ep
$F_2(p)$
1.5
1
0.5
0
0
1
2
3
4
5
μ
e
KMRS B- L=1000 pb^{-1}
$log Q^2/GeV^2$

$xG_3(x,Q^2)$: PROJECT OUT THE γZ- INTERFERENCE TERM.

$$\boxed{\begin{aligned} B_-(\lambda) &= \frac{1}{2}\,\frac{1}{Y_-(a-\lambda v)}\,\frac{1}{k_Z(Q^2)}\left[\sigma^+(-\lambda)-\sigma^-(+\lambda)\right] \\ &= xG_3(x,Q^2) + k_Z\,(-2va+\lambda(v^2+a^2))\,xH_3 \end{aligned}}$$

$\longrightarrow$ MEASUREMENT AT HIGH Q^2!

LEP1 × LHC $\mathcal{L} = 1000\,pb^{-1}$
LEP2 × LHC $\mathcal{L} = 100\,pb^{-1}$

HERA.

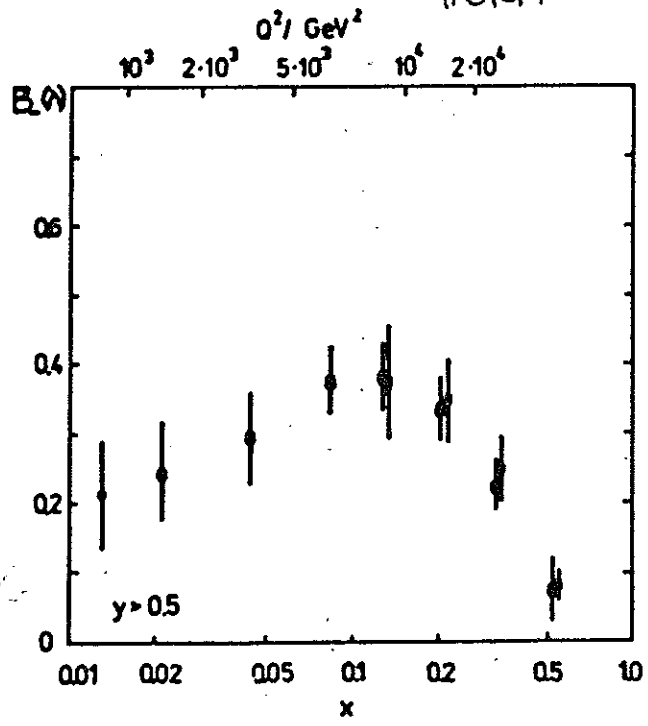

LEP × LHC

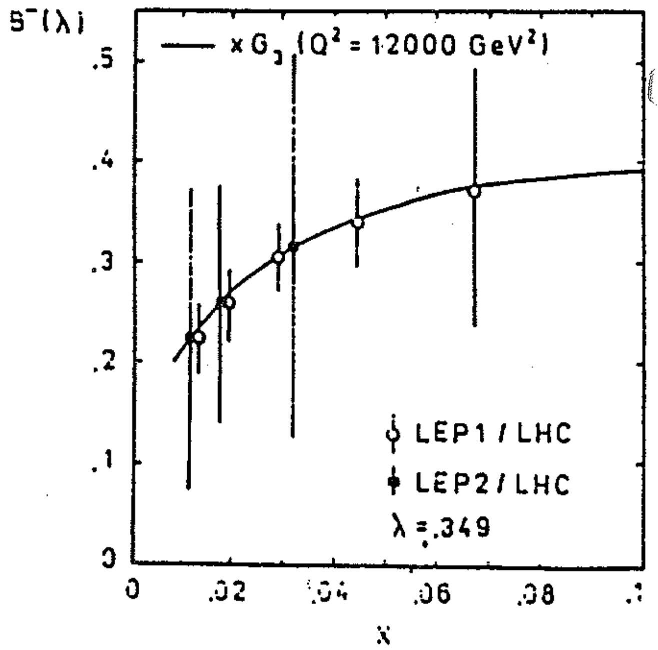

$xG_3(x,Q^2)$

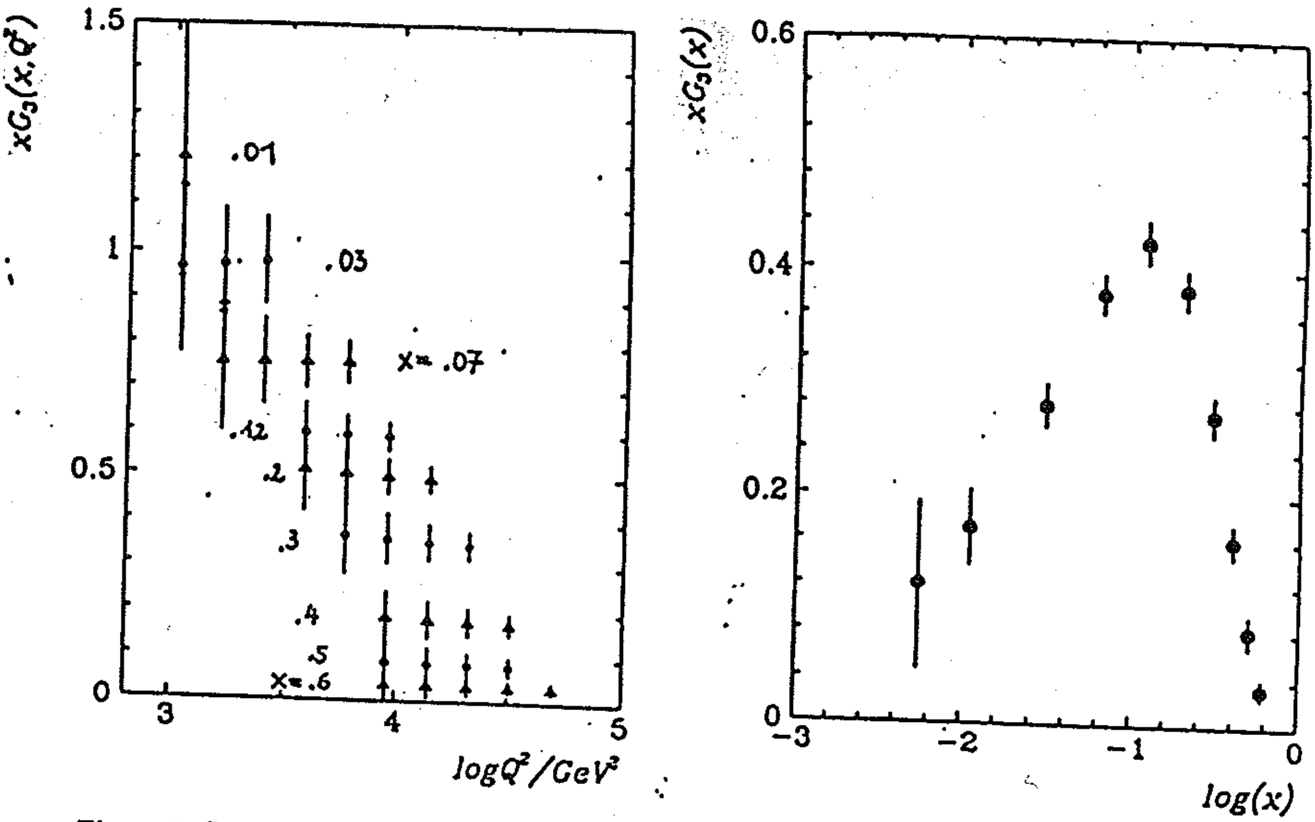

Figure 3: Statistical precision for a measurement of $xG_3(x,Q^2)$ (a) and of $xG_3(x)$ averaged over Q^2 in the accessible kinematical range (b) for $\mathcal{L} = 1\ fb^{-1}$

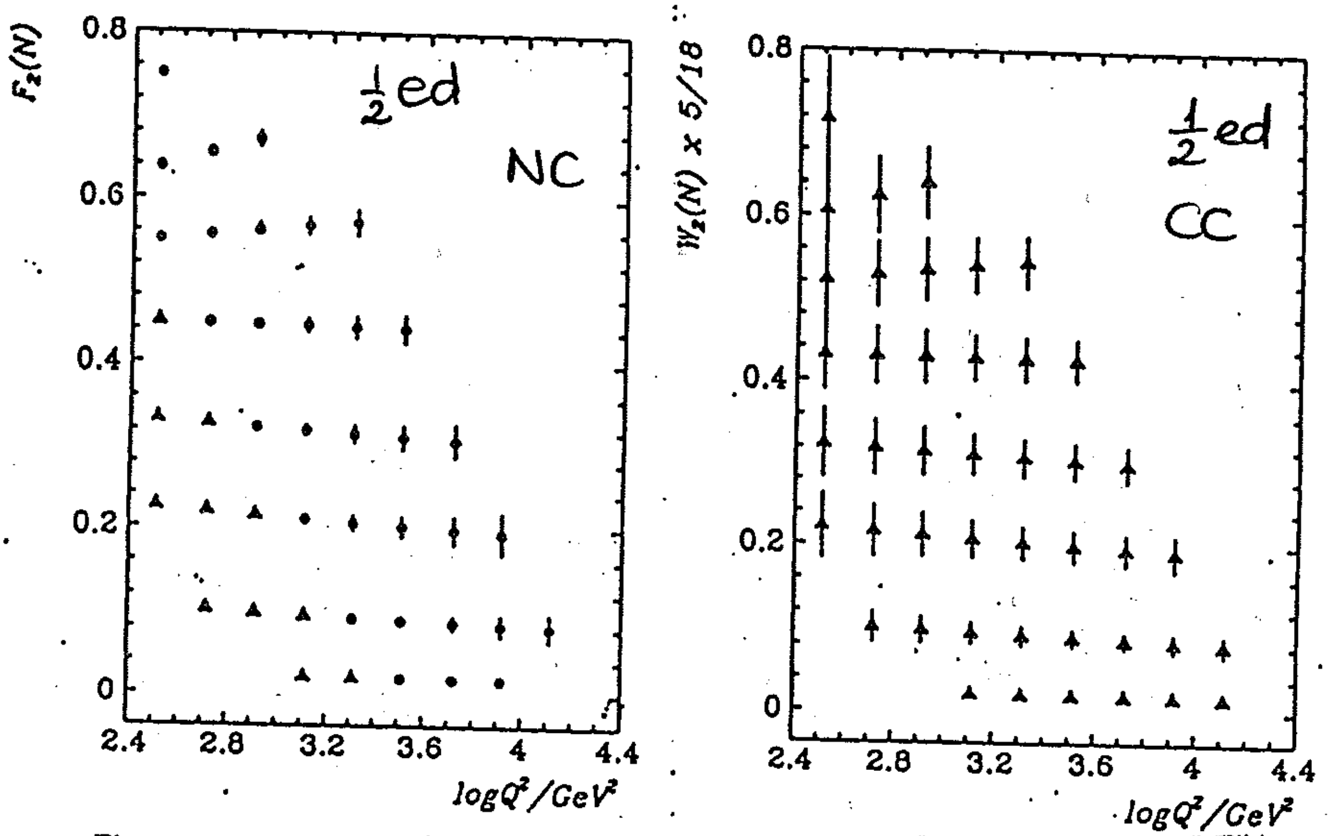

Figure 4: Statistical precision for a measurement with deuterons of F_2^{eN} and W_2^{eN}, for $\mathcal{L} = 100\ pb^{-1}$.

WAYS TO UNFOLD PARTON DENSITIES

$\boxed{e^{\pm}p}$ 4 CROSS SECTIONS $\sigma_{NC}^{\pm}, \sigma_{CC}^{\pm}$ $\hookrightarrow$ 4 COMBINATIONS OF PARTON DENSITIES

LINEAR MAPPING: $\overset{(-)}{U} = \sum_i x \overset{(-)}{u}_i \; ; \; \overset{(-)}{D} = \sum_i x \overset{(-)}{d}_i$

$$\boxed{\begin{pmatrix} U \\ \overline{U} \\ D \\ \overline{D} \end{pmatrix} = (A_{ij}) \begin{pmatrix} \sigma_{NC}^{-} \\ \sigma_{NC}^{+} \\ \sigma_{CC}^{-} \\ \sigma_{CC}^{+} \end{pmatrix}}$$

$$\det{}_4 A_{ij} \sim \left\{ \kappa_Z(Q^2)\, [1-(1-y)^4] \right\}^{-1}$$

(A_{ij}) becomes singular (degenerate) both for: $Q^2 \ll M_Z^2$, $y \ll 1$

CONSIDER e.g. (WITH ASSUMPTIONS ON SEA-QUARKS)

$$\boxed{\begin{pmatrix} x u_v \\ x d_v \\ x s \end{pmatrix} = (B_{ij}) \begin{pmatrix} \sigma_{NC}^{-} \\ \sigma_{NC}^{+} \\ \sigma_{CC}^{-} \end{pmatrix}}$$

APPROXIMATE REPRESENTATIONS

VALENCE RANGE

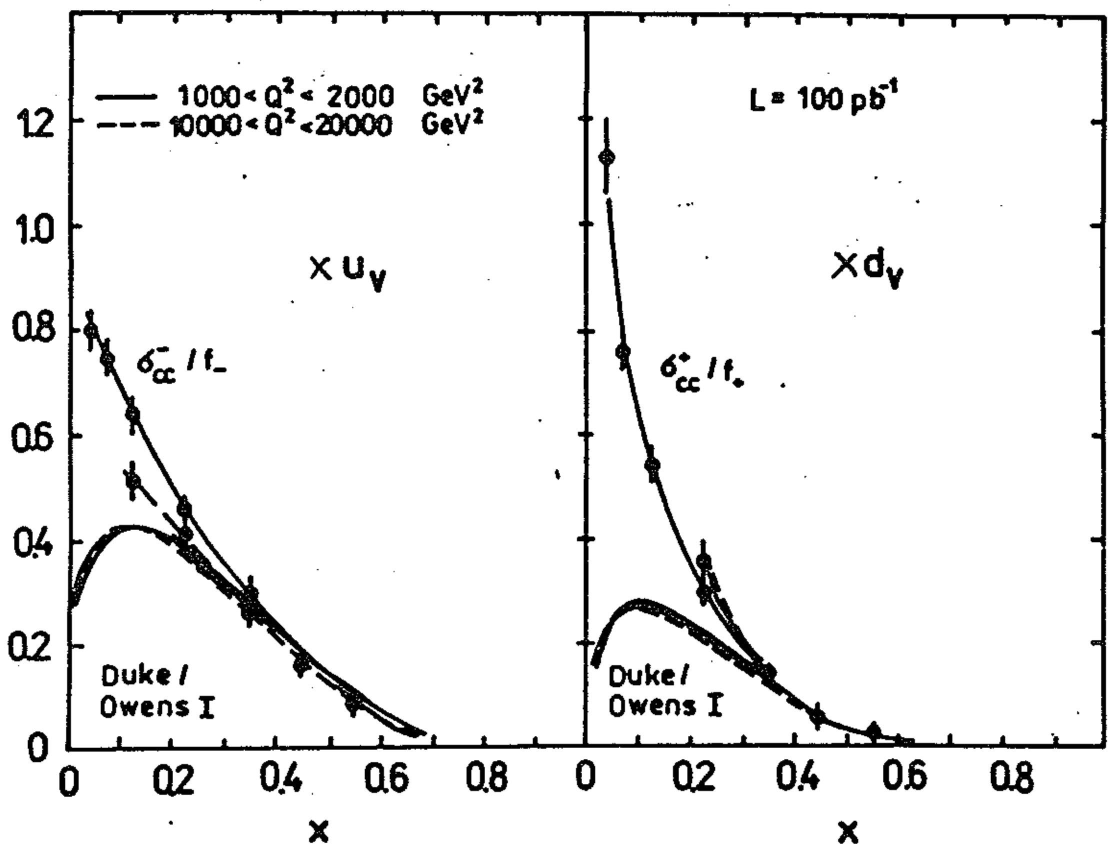

$$f_\pm = \frac{1}{2}(Y_+ \mp Y_-)\, K_W^2$$

$\mathcal{L} = 100\,pb^{-1}$

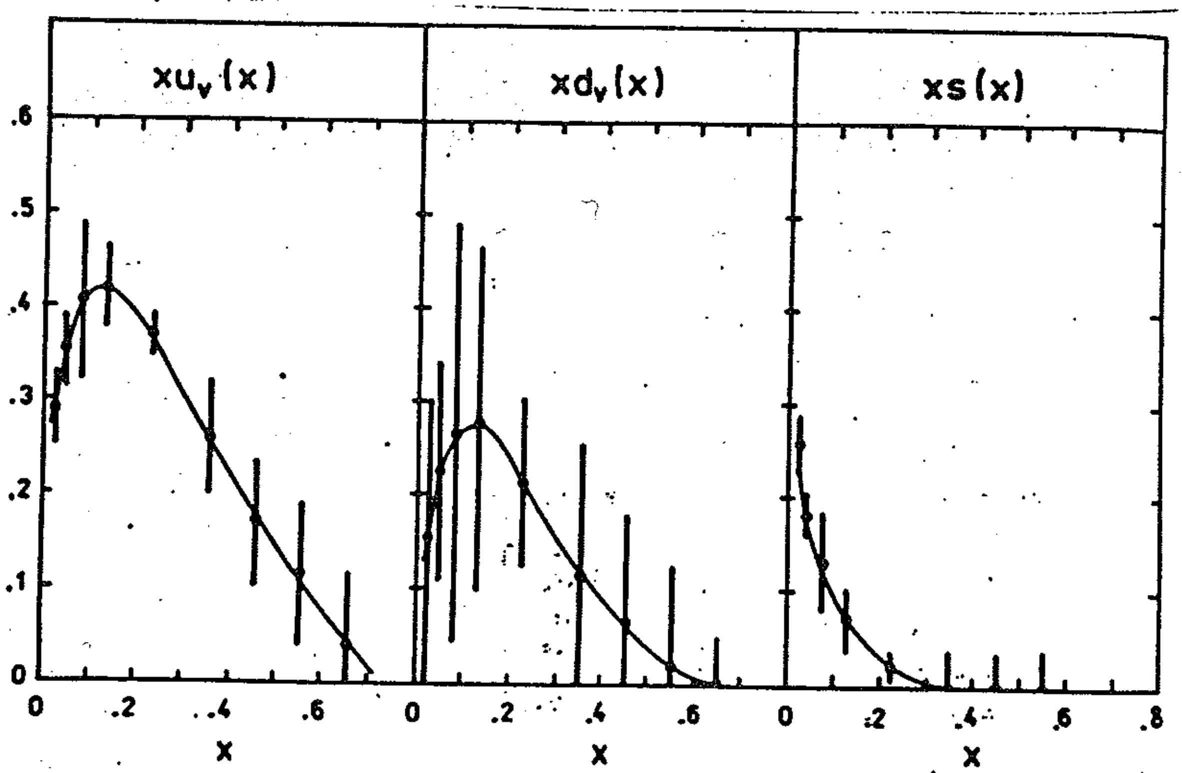

$\mathcal{L} = 100 pb^{-1}$ / per beam

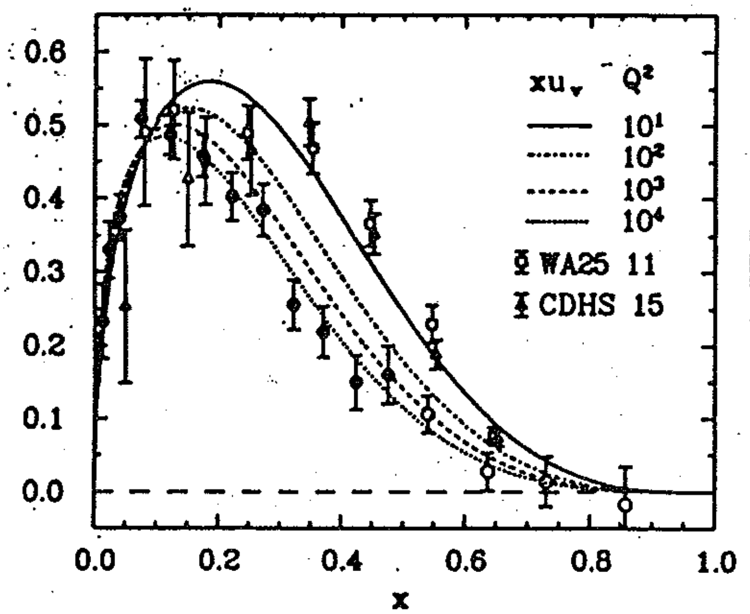

Ingelman / Rückl

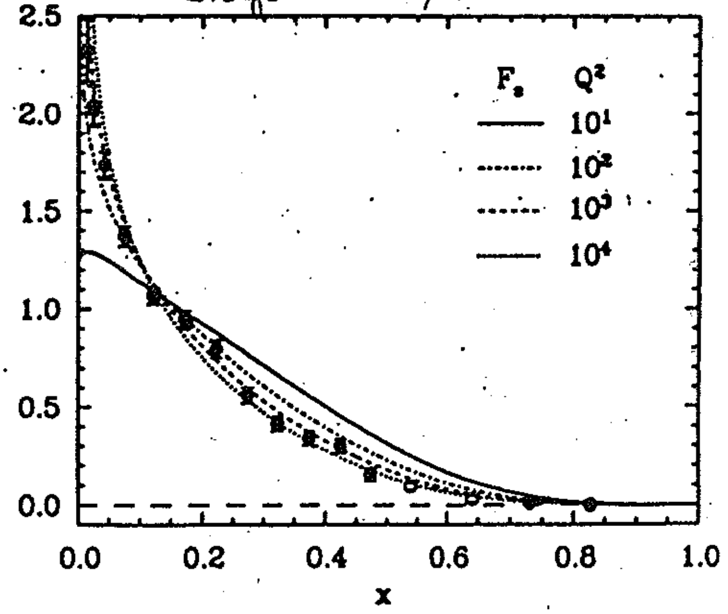

$\Sigma \mathcal{L} = 400 pb^{-1}$

$e^{\pm}p$ & $e^{\pm}d$

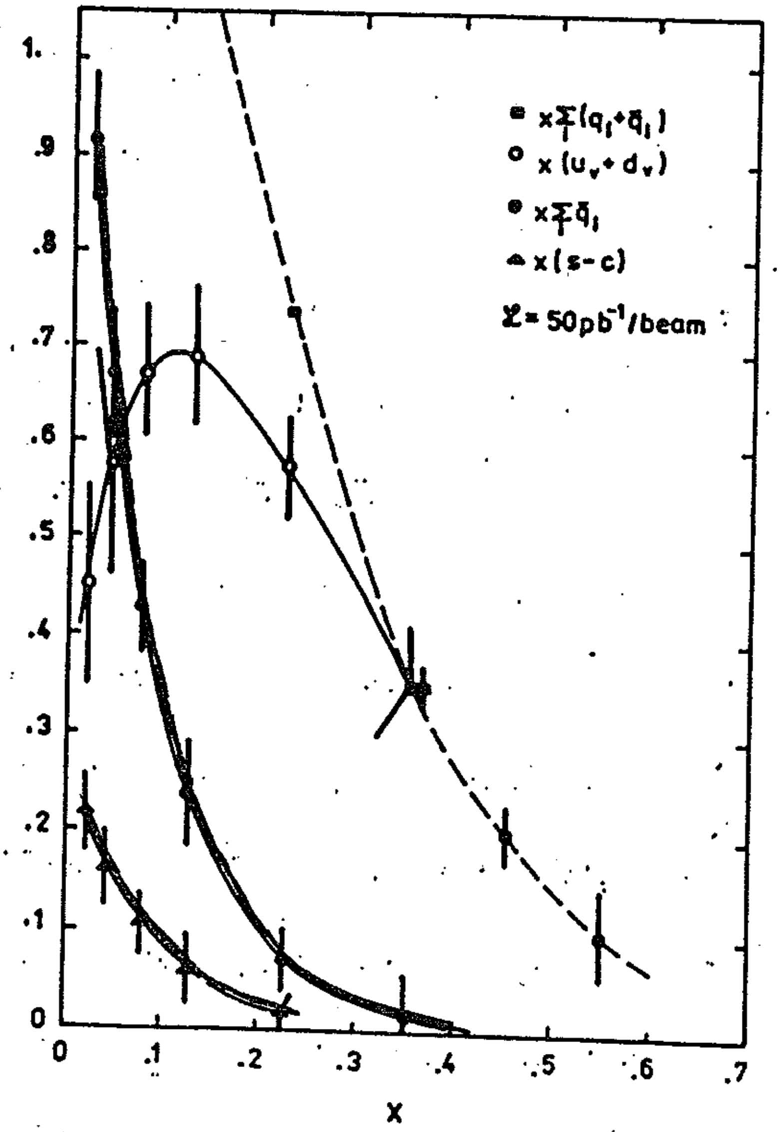

$$\overline{Q} = \frac{1}{2}\left(W_2^{eN} - x W_3^{eN}\right)$$

$$X(s-c) = \frac{5}{18} W_2^{eN} - F_2^{eN} \quad , \quad b \approx 0$$

$\mathcal{L} = 50 pb^{-1}/beam$

ACCESS TO THE GLUON: F_L, $\sigma_{J/\psi}$, $\sigma_{c\bar{c}}$ ...

SO FAR: ACCESS TO QUARKS ONLY.

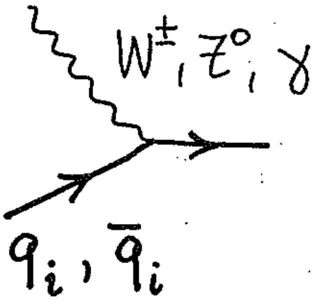

GLUONS

1) 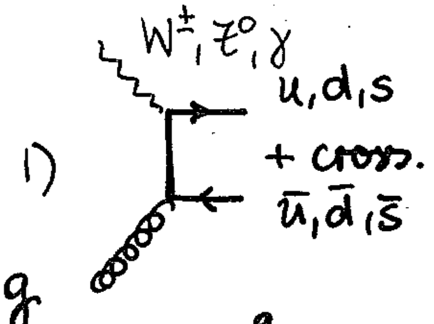

F_L^g

2) 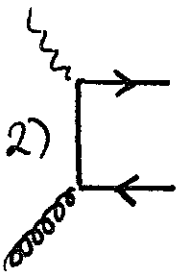

NC		CC	
c	b	(c)	(c)
$\bar{c}$	$\bar{b}$	(s)	(b)

heavy flavour cross sections

3) 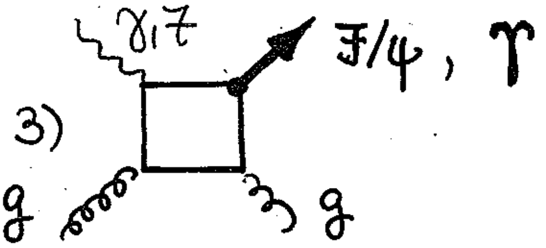

4) SCALING VIOLATIONS: next paragraph.

MARTIN, ROBERTS, STIRLING

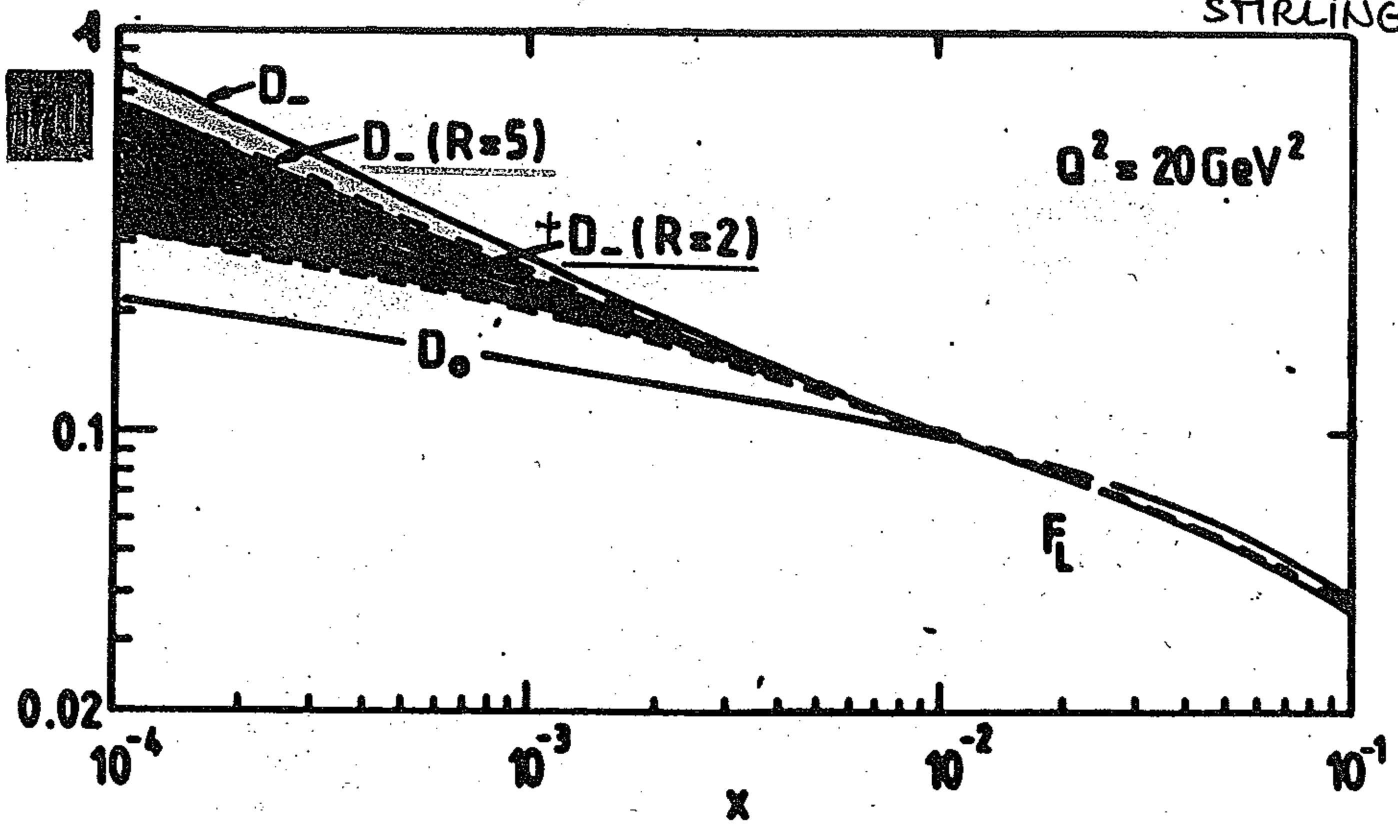

$O(\alpha_s)$:

$$Q^2 = x(ys)$$

$$F_L(x,Q^2) = \frac{\alpha_s}{2\pi}\left\{\frac{8}{3}\int_x^1 \frac{dy}{y}\left(\frac{x}{y}\right)^2 F_2(y,Q^2) + 2\sum_{q,\bar{q}} e_q^2 \int_x^1 \frac{dy}{y}\left(\frac{x}{y}\right)^2\left(1-\frac{x}{y}\right) y\, \underline{G(y,Q^2)}\right\}$$

ROBERTS:

$$xG(x,Q^2) \simeq \frac{3}{5}\times 5.85\left\{\frac{3\pi}{4\alpha_s} F_L(0.4x,Q^2) - \frac{1}{2} F_2(0.8x,Q^2\right\}$$

LO QCD

HERA

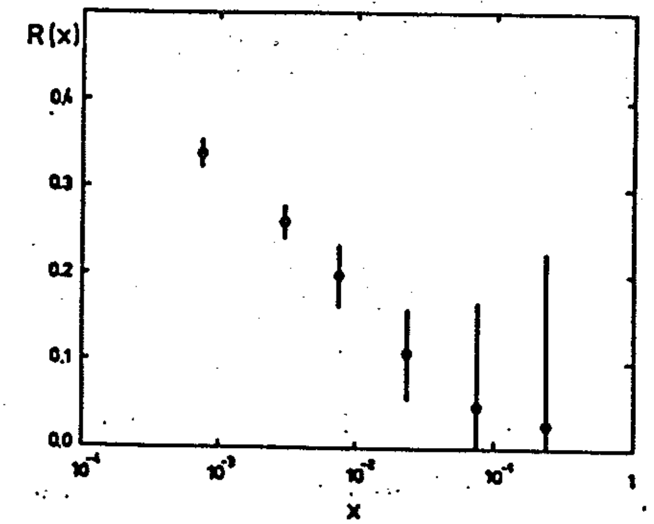

UNK

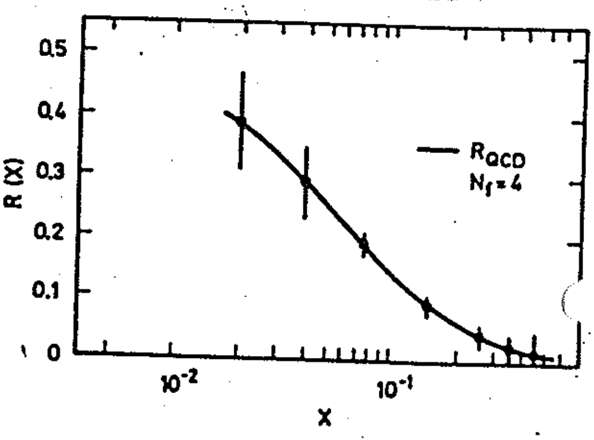

Fig. 11. Possible measurement of $R(x)$ using Eq. (6.1)

'y'-DEPENDENCE (INVARIANCE)

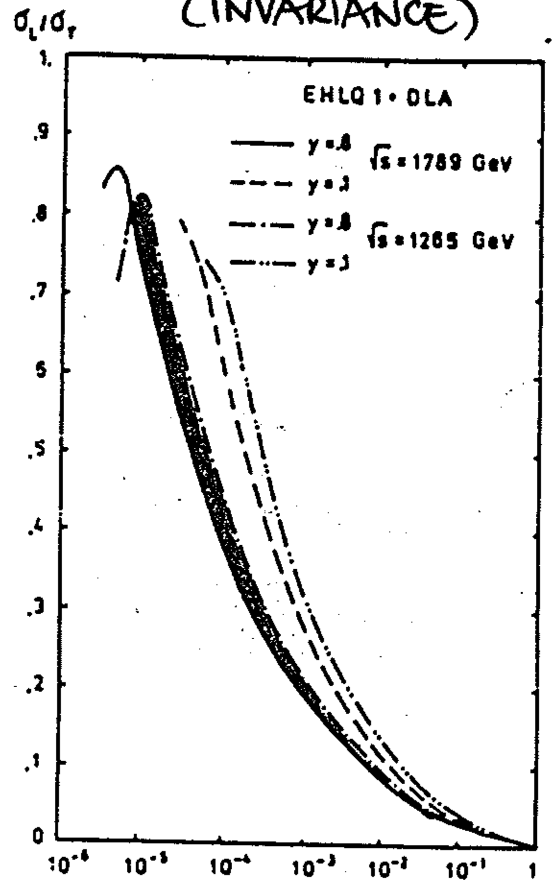

LEP × LHC

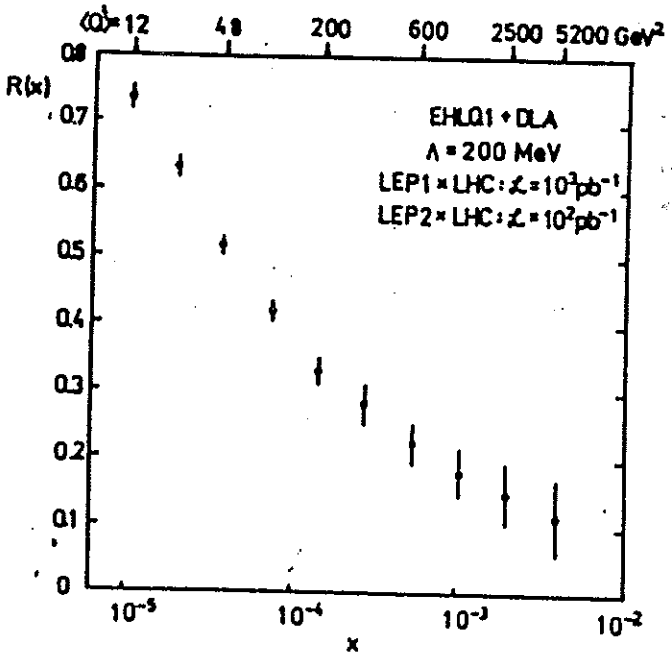

$$xG(x,Q^2) \simeq 1.77 \frac{3\pi}{2\alpha_s(Q^2)} F_L(0.4x, Q^2)$$

HERA

OXFORD GROUP

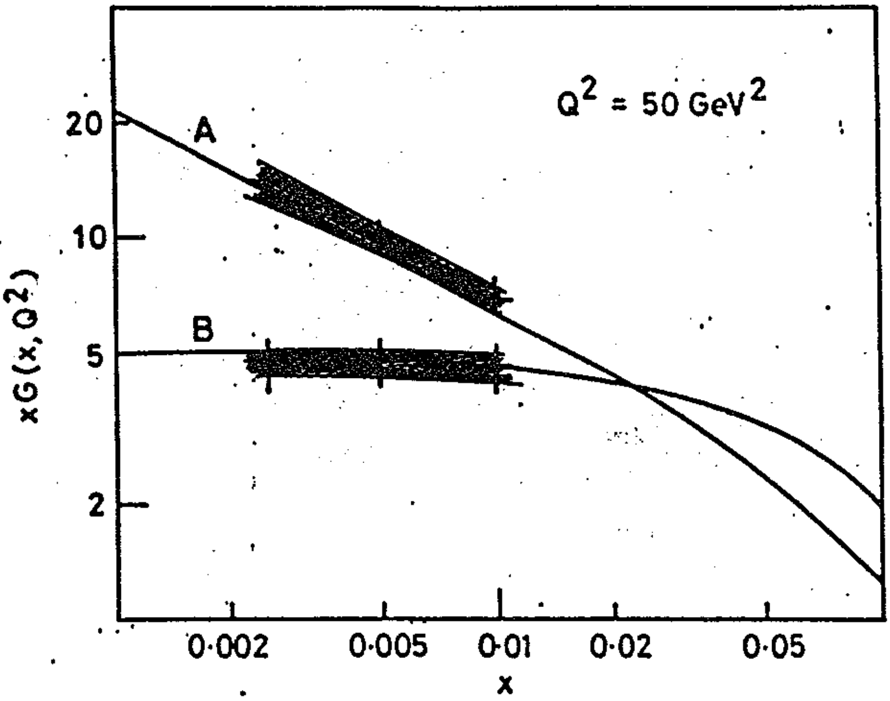

FIG. 8a

JB

LEP / LHC

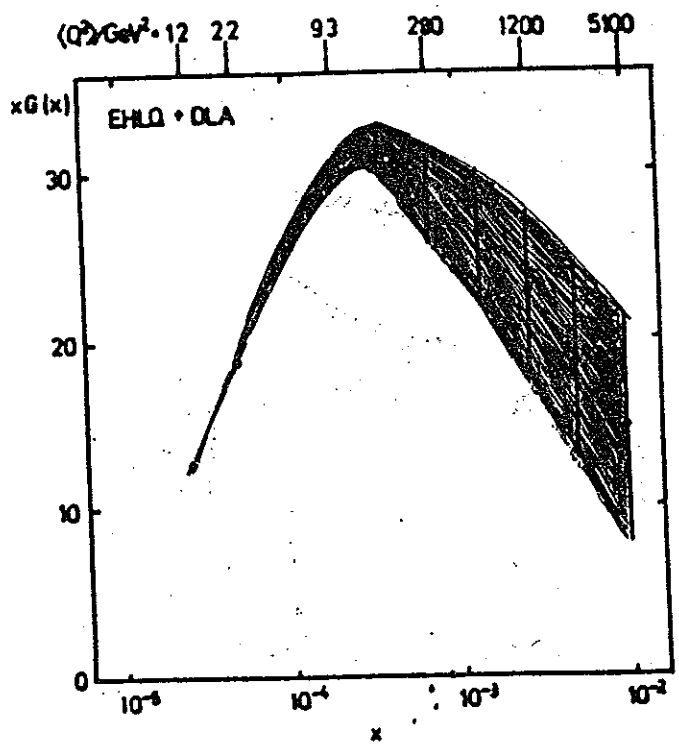

Figure 4: Statistical precision of a possible measurement of $xG(x)$

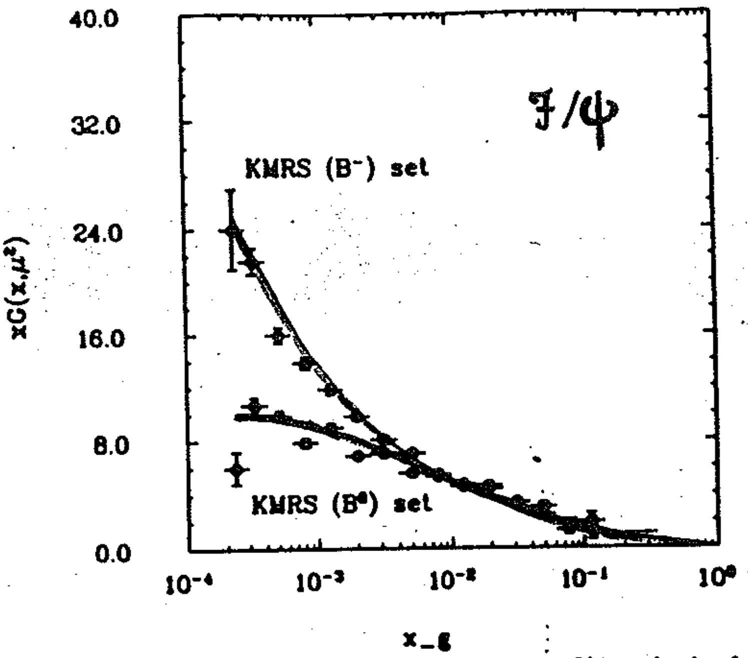

JUNG et al.

$Q^2 \approx M^2_{J/\psi}$

Figure 16: The gluon density reconstructed from inelastic J/ψ production for the input function of KMRS. The statistical error bars correspond to an integrated luminosity of 100 pb^{-1}. The curves show the input gluon density.

PROBLEMS: • WF's
• K-factor

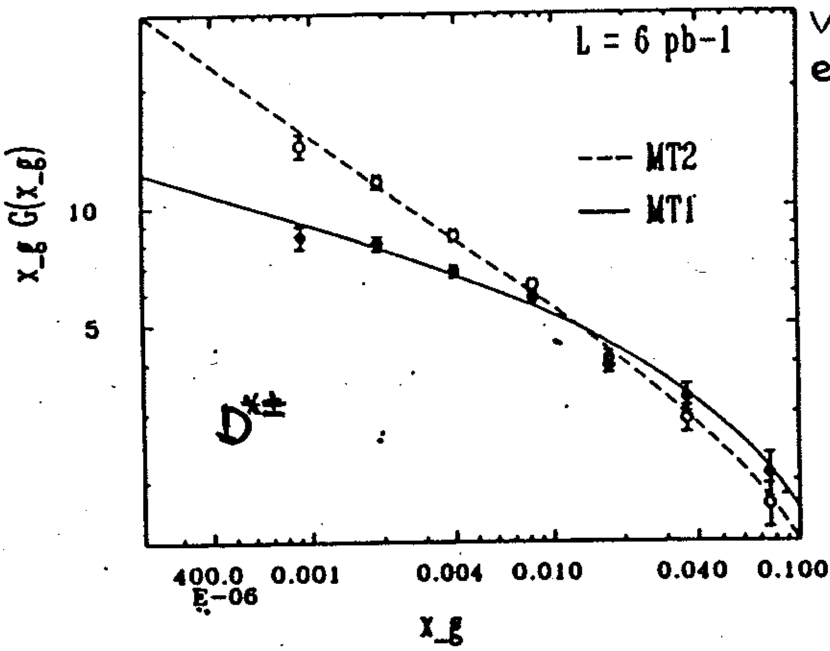

VAN WOUDENBERG et al.

PROBLEMS:
→ DECAY BG.
→ FRAGMENTAT.
→ SCALE !

Figure 18

Reconstructed gluon densities from inclusive $D^{*\pm}$ production. The curves show the input gluon functions taken from Morfin and Tung [36]. The error bars include statistical errors for an integrated luminosity of 6 pb^{-1}.

$e^{\pm}p$: GENERAL SITUATION

$$\boxed{\begin{aligned} B_+(x,Q^2) &= C_\Sigma(Q^2)\,\Sigma(x,Q^2) + C_\Delta(Q^2)\,\Delta(x,Q^2) \\ &= C_\Sigma(Q^2)\Big[E_{qq}(x,Q^2)\otimes\Sigma(x,Q_0^2) \\ &\qquad + E_{gq}(x,Q^2)\otimes G(x,Q_0^2)\Big] \\ &\quad + C_\Delta(Q^2)\,E_{NS}(x,Q^2)\otimes\Delta(x,Q_0^2) \end{aligned}}$$

$$Q^2/M_Z^2 \to 0 \;:\quad C_\Sigma \to \frac{5}{18}\;,\quad C_\Delta \to \frac{1}{6}$$

VALENCE RANGE :

$$\begin{aligned} B_+^{VAL}(x,Q^2) &= C_\Sigma(Q^2)\otimes E_{qq}(x,Q^2)\otimes\Sigma^{val}(x,Q_0^2) \\ &\quad + C_\Delta(Q^2)\otimes E_{NS}(x,Q^2)\otimes\Delta^{val}(x,Q_0^2). \end{aligned}$$

for $C_\Sigma \simeq 5/18$, $C_\Delta \simeq 1/6$ & LO : $E_{qq} \equiv E_{NS}$

$$\boxed{B_+^{VAL}(x,Q^2) = E_{NS}(x,Q^2)\otimes\left[\frac{5}{18}\,\Sigma^{val}(x,Q_0^2) + \frac{1}{6}\,\Delta^{val}(x,Q_0^2)\right]}$$

$e^{\pm}p\ (d)$

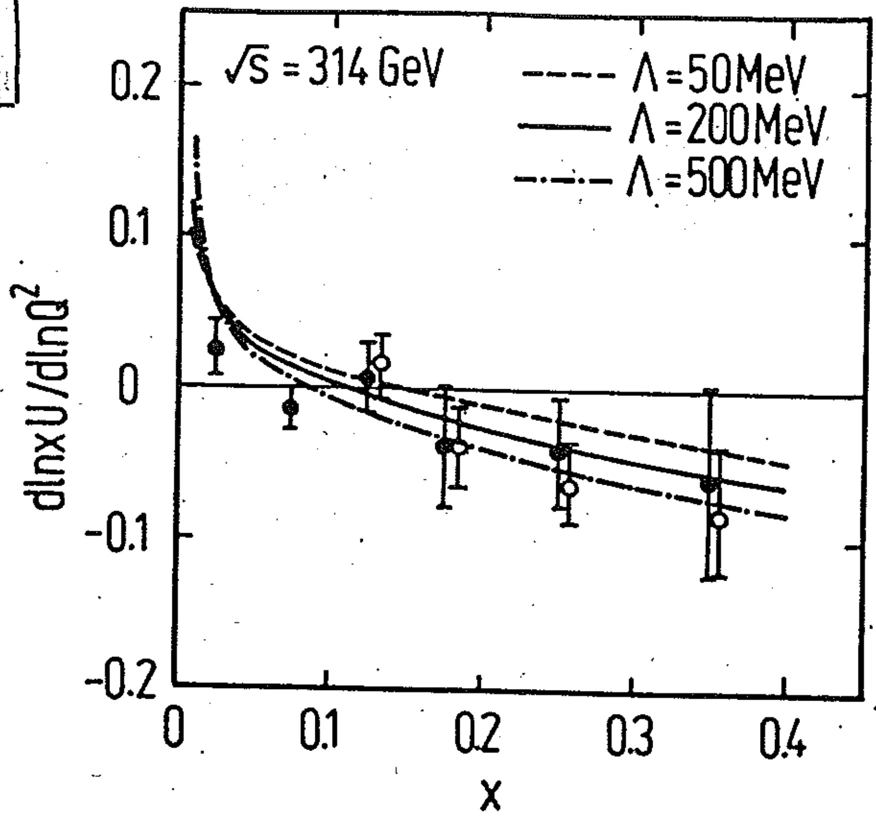

TOO LARGE ERRORS TO ALLOW A QCD ANALYSIS

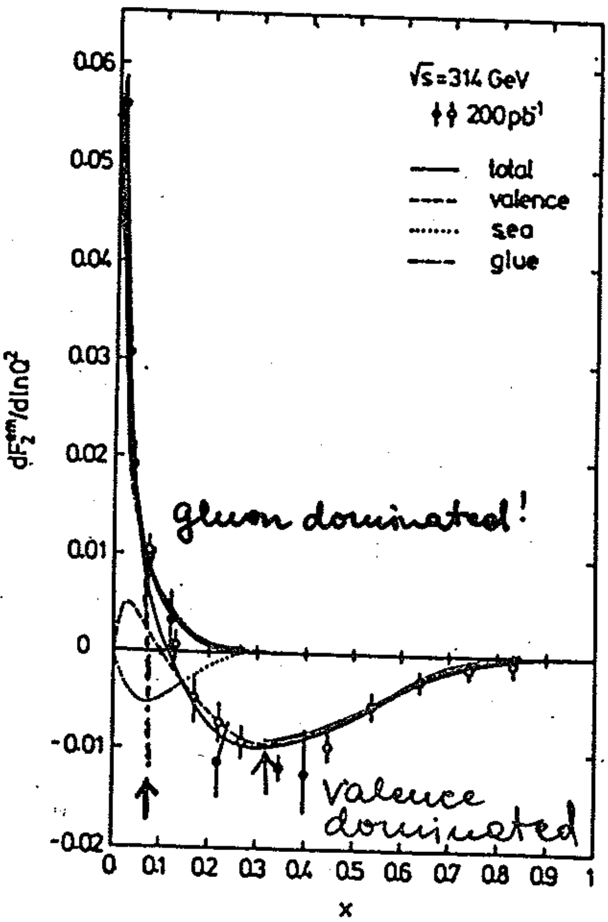

F_2^{em} !

$$\boxed{\frac{\partial E_{NS}(x,Q^2)}{\partial \log Q^2} = \frac{\alpha_s(Q^2)}{2\pi} C_F \; P_{qq}(x) \otimes E_{NS}(x,Q^2)}$$ NS

LO SPLITTING FUNCTIONS:

$$P_{qq}(x) = C_F\left[\frac{1+x^2}{(1-x)_+} + \frac{3}{2}\delta(1-x)\right]$$

$$P_{gq}(x) = C_F \frac{1+(1-x)^2}{x}$$

$$P_{qg}(x) = T_R\left[x^2+(1-x)^2\right]$$

$$P_{gg}(x) = 2N_c\left[x(1-x) + \frac{1-x}{x} + \frac{x}{(1-x)}\right]_+ + \delta(1-x)\cdot\frac{1}{2}\beta_0$$

$C_F = 4/3$, $T_R = 1/2$, $N_c = 3$, $\beta_0 = 11/3 \cdot N_c - 4/3\, N_F T_R$.

$$\frac{\partial}{\partial \log Q^2}\begin{pmatrix} E_{FF} & E_{FG} \\ E_{GF} & E_{GG} \end{pmatrix} = \begin{pmatrix} P_{qq} & N_f\, P_{qG} \\ P_{Gq} & P_{GG} \end{pmatrix} \otimes \begin{pmatrix} E_{FF} & E_{FG} \\ E_{GF} & E_{GG} \end{pmatrix}$$

SINGLET

SIMILAR STRUCTURE IN NTLO:

$$P_{ij}(x,Q^2) = P_{ij}^{(0)}(x) + \frac{\alpha_s}{2\pi} P_{ij}^{(1)}(x) + \dots$$

Q9/1

$e^{\pm}p$

HERA

$\frac{\partial \ln F_2}{\partial \log Q^2}$

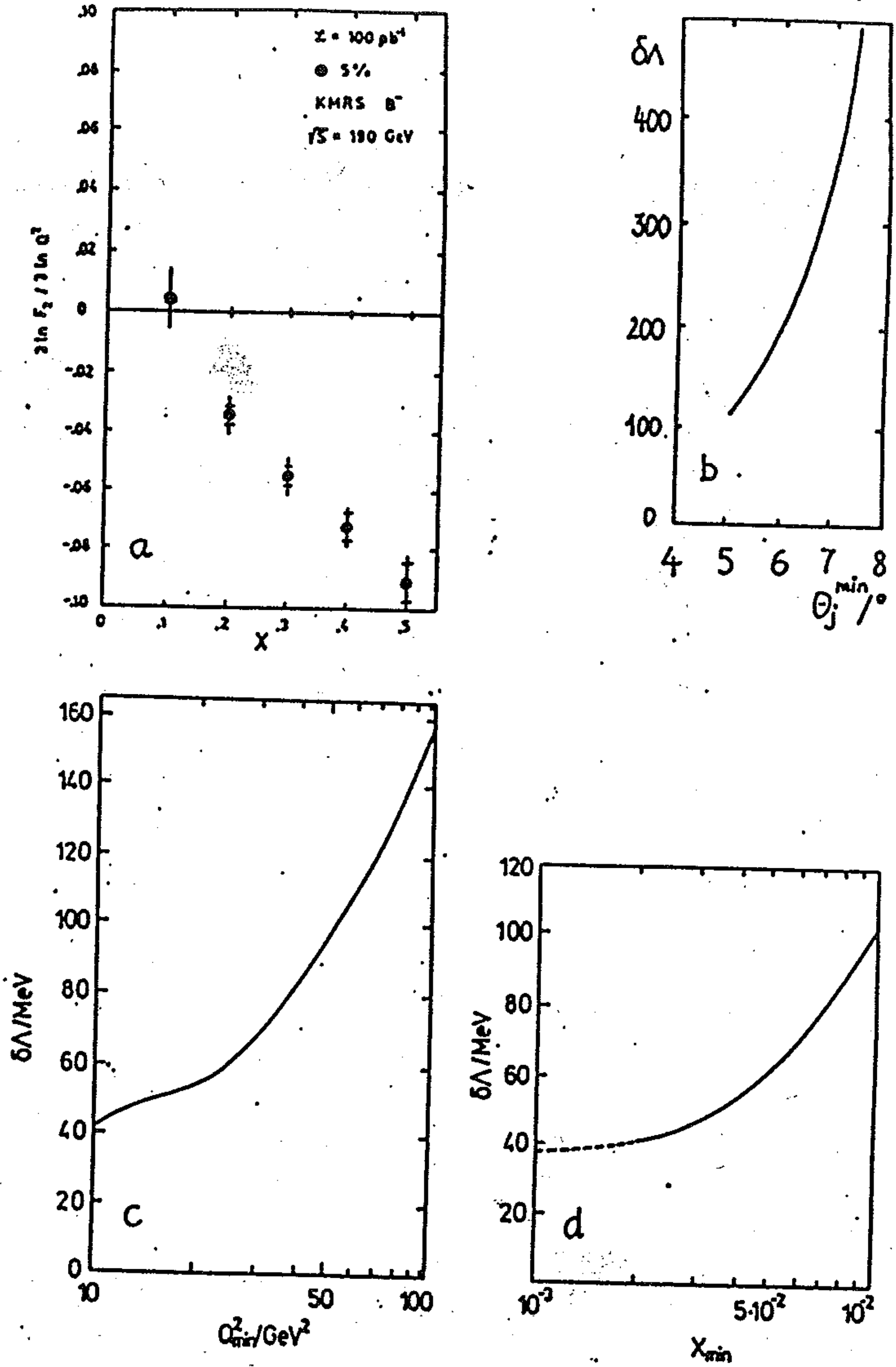

Figure 6: (a) Average slope $(\partial F_2/\partial \ln Q^2)$ *versus* x using the KMRS distribution B^- in the valence range. The inner error bars represent the statistical error for 100 pb^{-1} with a systematical error of 5% superimposed. (b) Dependence of $\delta\Lambda_{stat}$ for $x \geq 0.25$ 100 pb^{-1} and $\sqrt{s} = 110$ GeV on the minimum jet angle. Dependence of $\delta\Lambda_{stat}$ on the minimum Q^2 (c) and x (d) used in the QCD fit for the combined data sets at $\sqrt{s} = 110$ and 314 GeV for $\mathcal{L} = 100$ pb^{-1} each.

JB, M.KLEIN

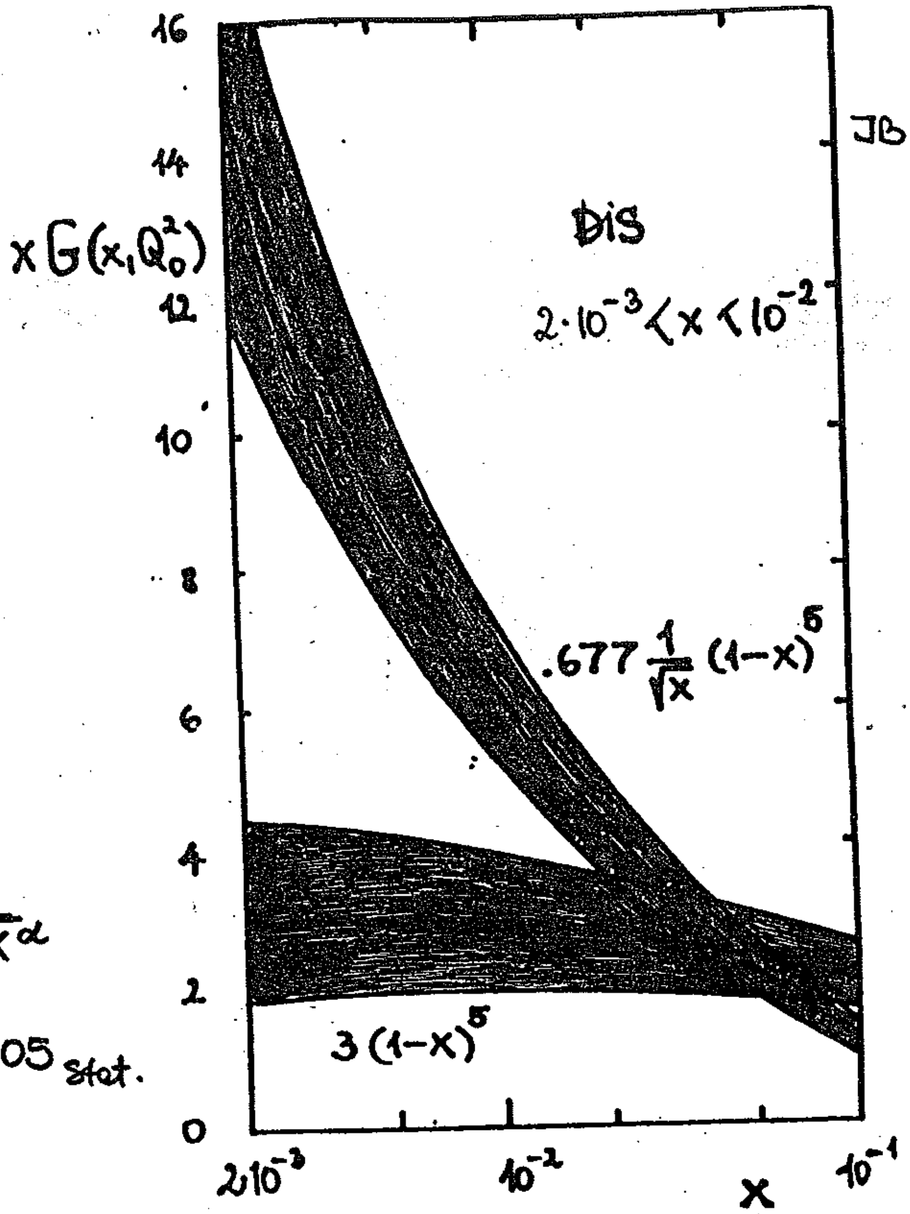

$xG \propto \frac{1}{x^\alpha}$

$\delta\alpha \simeq \pm 0.05_{stat.}$

Figure 8: Possible determination of $xG(x, Q_0^2)$ in a QCD fit for $x < 0.1$, see text. The upper error band corresponds to the choice $\alpha = -0.5$ and the lower band to $\alpha = 0$, see eq. 15. The inner error denotes the statistical error for $\mathcal{L} = 100\ pb^{-1}$ for both the low and high s option.

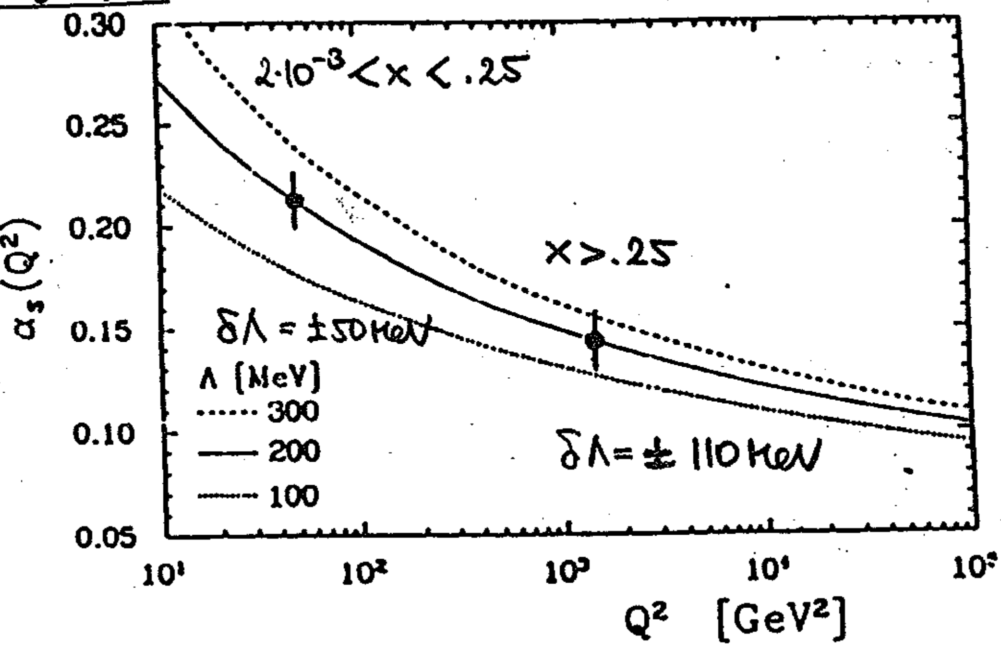

Figure 7: Dependence of α_s on Q^2 from a combined fit using two samples of $\sqrt{s} = 314$ GeV and $\sqrt{s} = 110$ GeV with $\mathcal{L} = 100\ pb^{-1}$ each. The upper point corresponds to a nonsinglet fit for $\theta_j > 5°$ and $x > 0.25$. The lower point at $Q^2 \sim 50$ GeV^2 corresponds to a fit in the

5. FIRST RESULTS FROM HERA: DIS AT ZEUS & H1

	ZEUS	H1
LUMINOSITIES:	$\mathcal{L} = 2{,}1\,nb^{-1}$	$1{,}3\,nb^{-1}$

NEW DATA $\longrightarrow$ $*\,10$

$E_e = 26.7$ GeV

$E_p = 820$ GeV

$5 \lesssim Q^2 \lesssim 50$ GeV^2 dominantly, $Q^2_{max} \sim 800\,GeV^2$

$10^{-4} \lesssim x \lesssim 10^{-2}$

27.11.92, H1: $Q^2 = 2600\,GeV^2$

now, already higher Q^2 probed.

H1

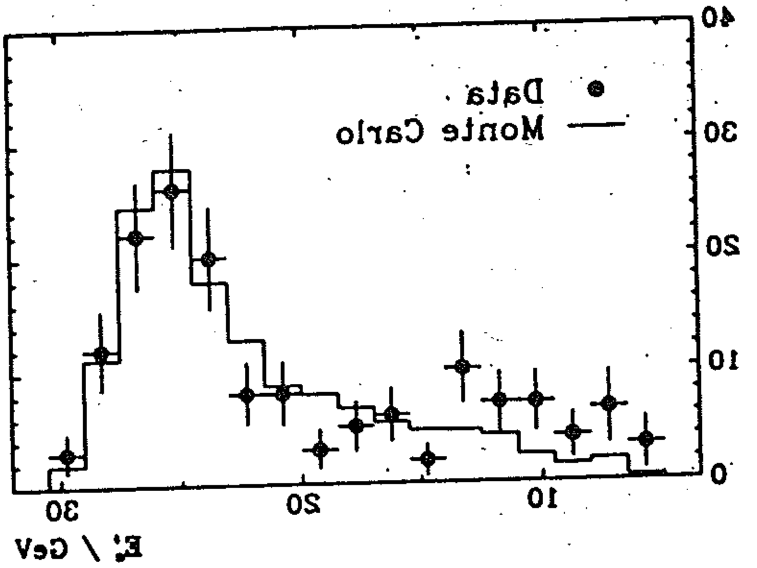

Figure 3: Electron energy spectrum of the DIS events compared with a Monte Carlo simulation [13,14] of the H1 detector using the parametrisation MRSD0 [15]. The simulated spectrum is normalised to the measured integrated luminosity of 1.3 nb^{-1}.

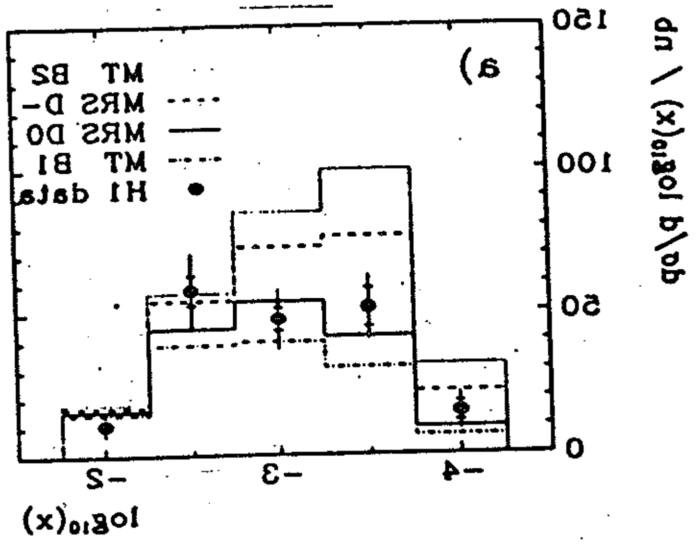

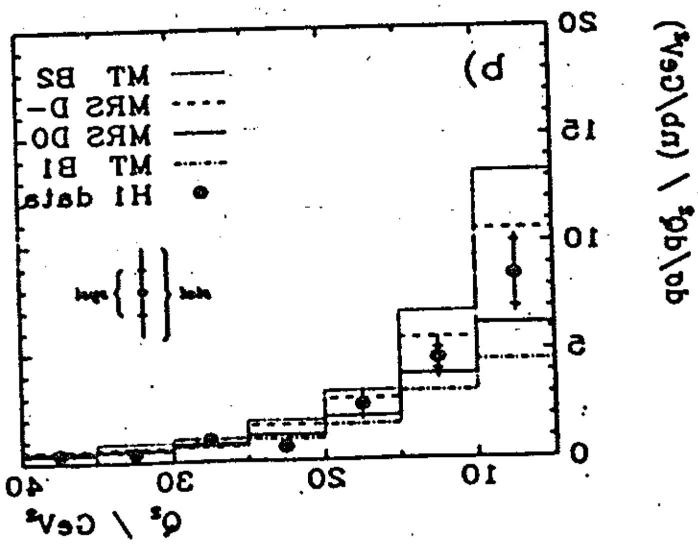

E3

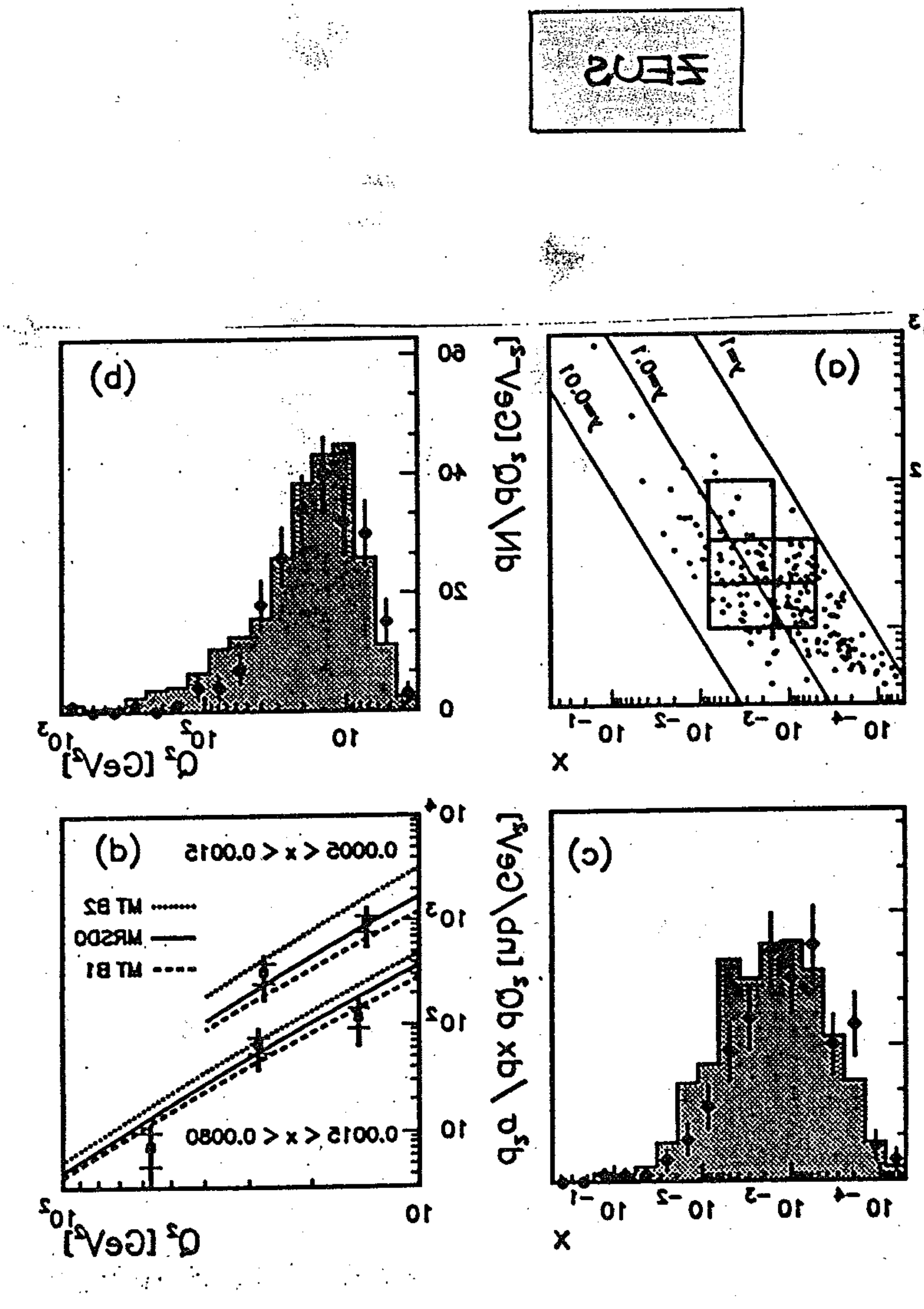

ZEUS
(a)
(b)
(c)
(d)
x
Q^2 [GeV^2]
dN/dQ^2 [GeV^{-2}]
dN/dx
$d^2\sigma$ / dx dQ^2 [nb/GeV^2]
y=1
y=0.1
y=0.01
0.0005 < x < 0.0015
0.0015 < x < 0.0080
MT B1
MRSD0
MT B2

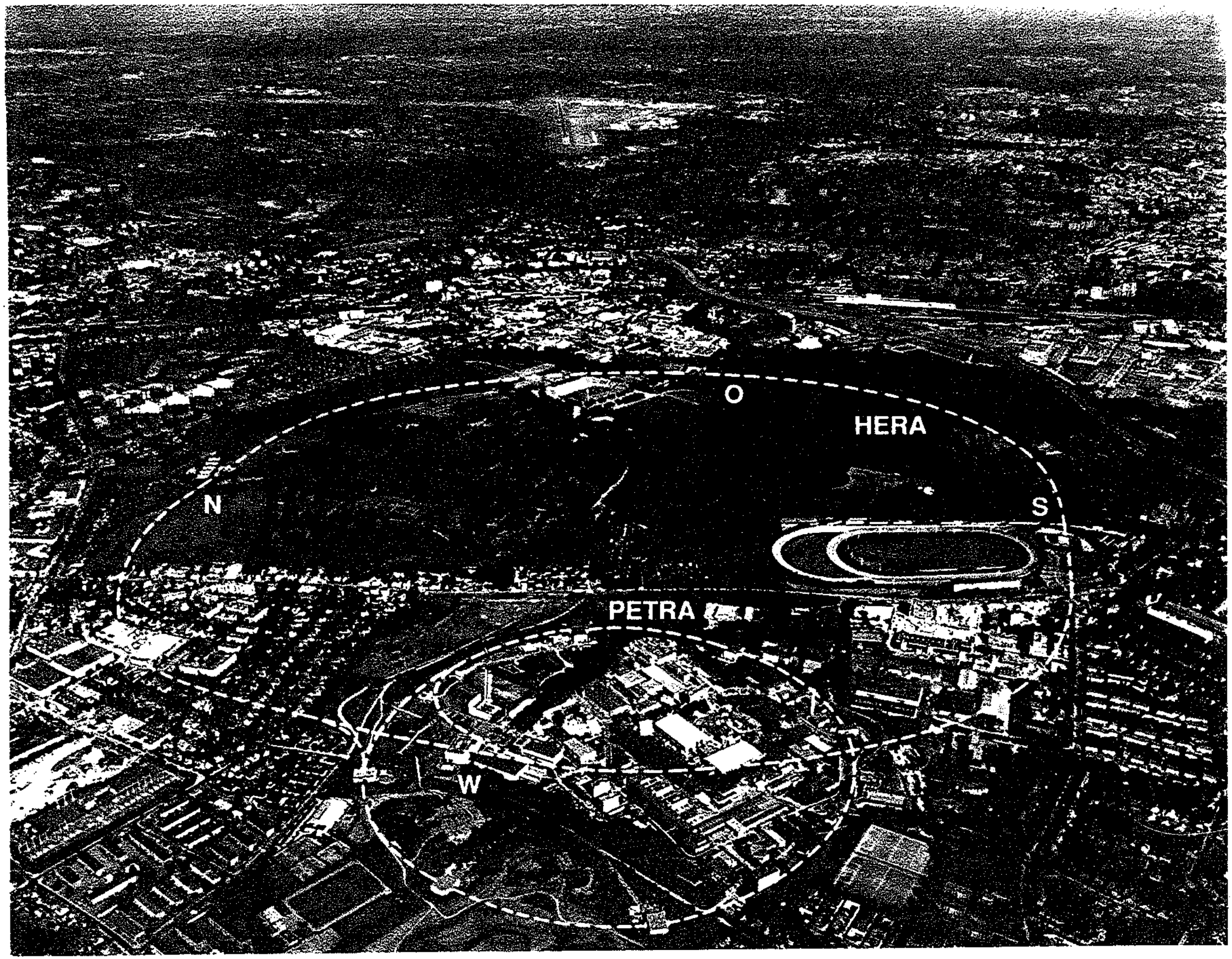
HERA
PETRA
O
N
S
W

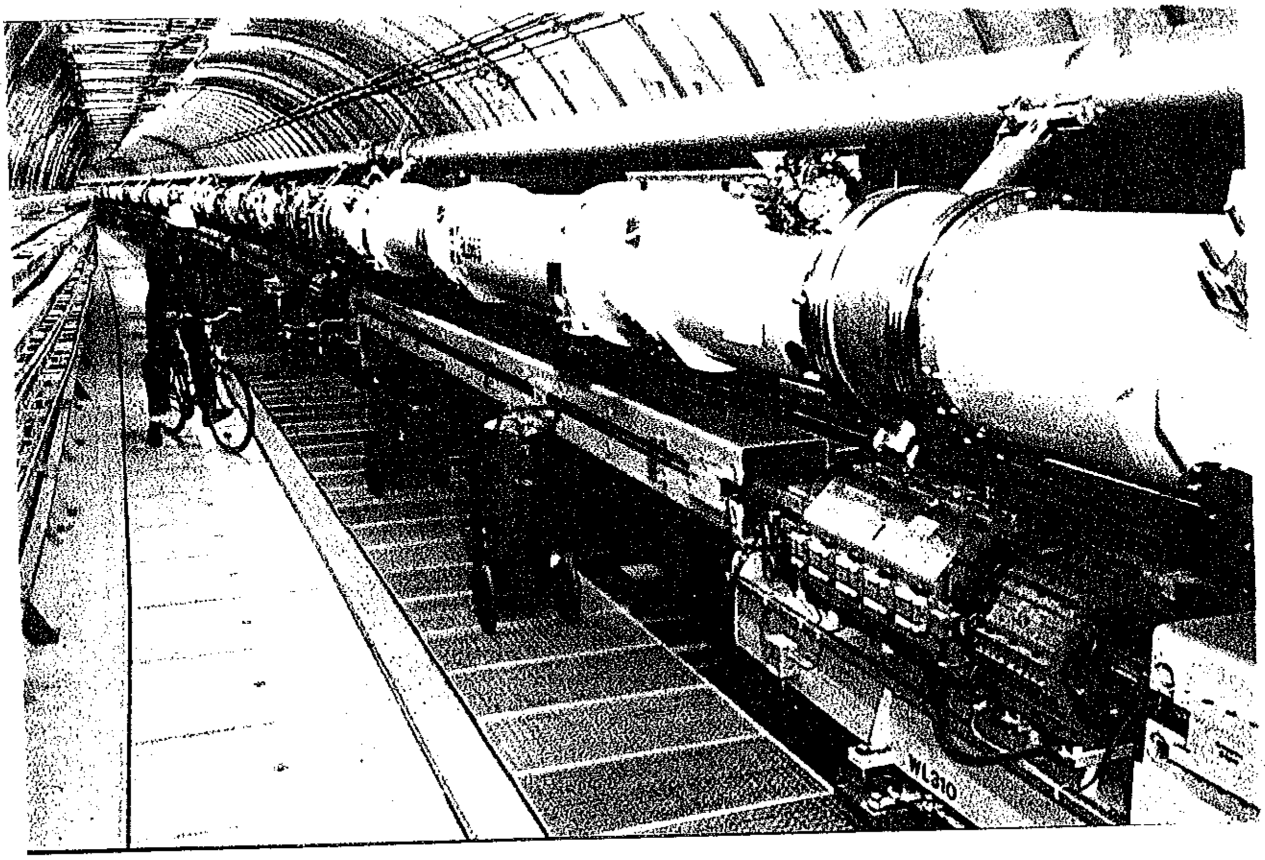
WL310

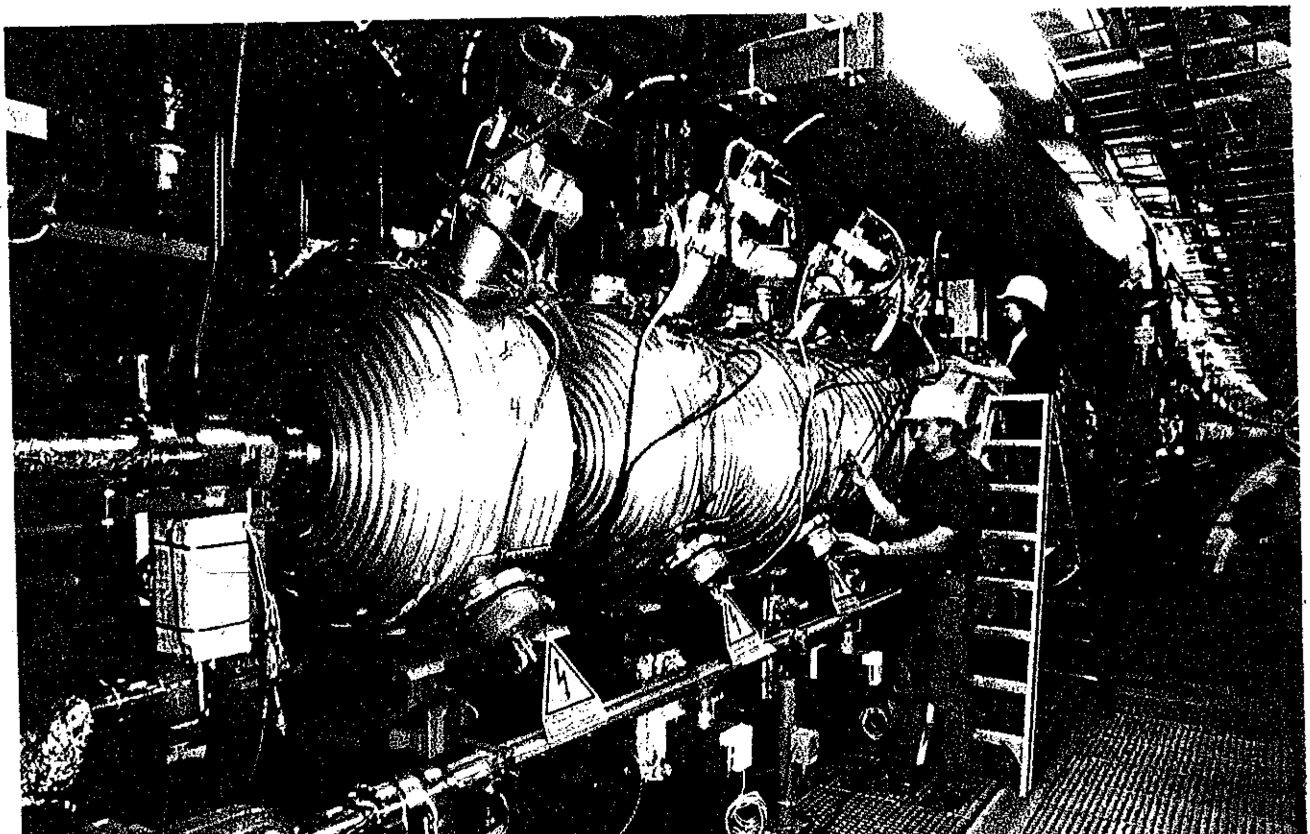

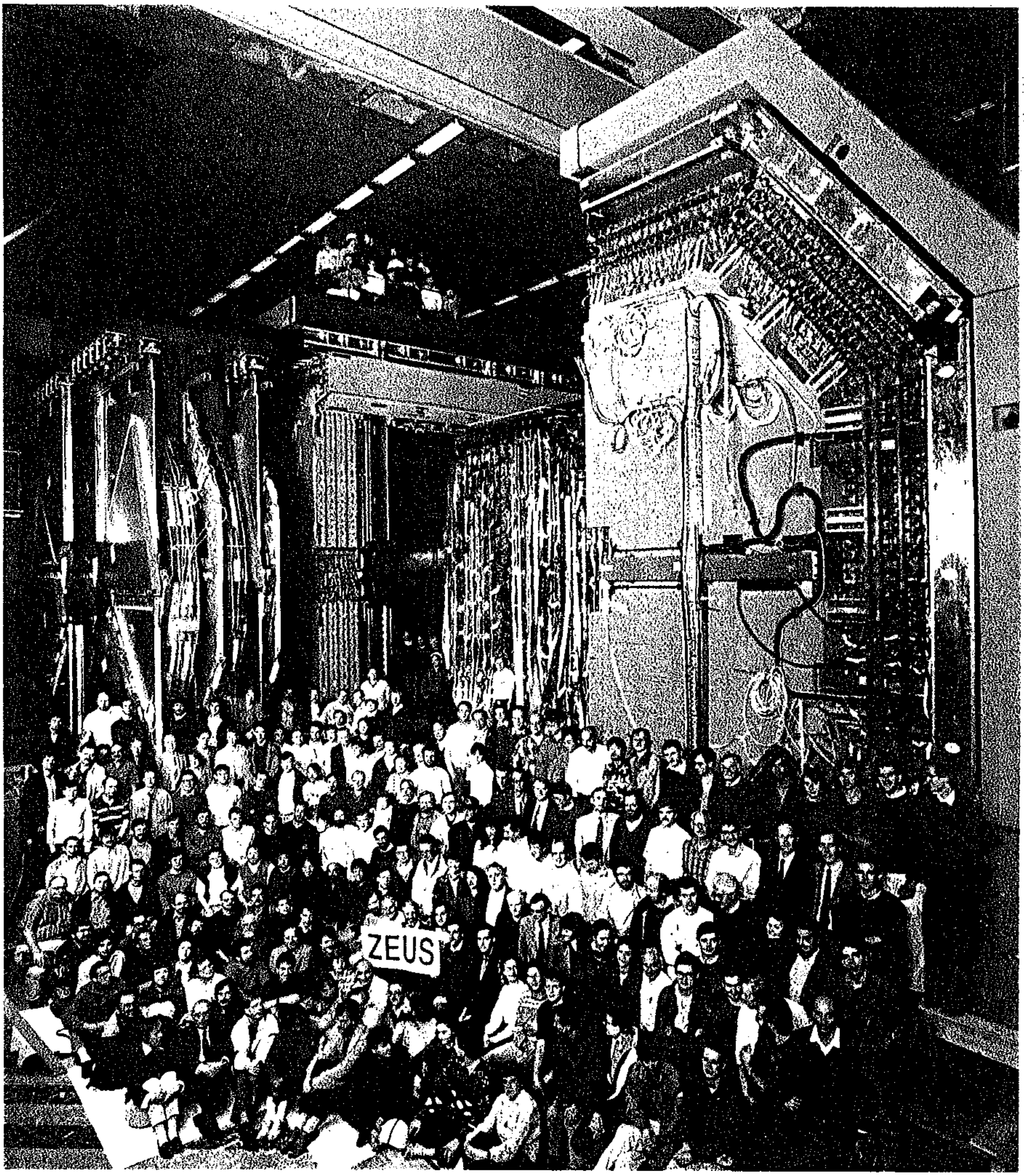
ZEUS

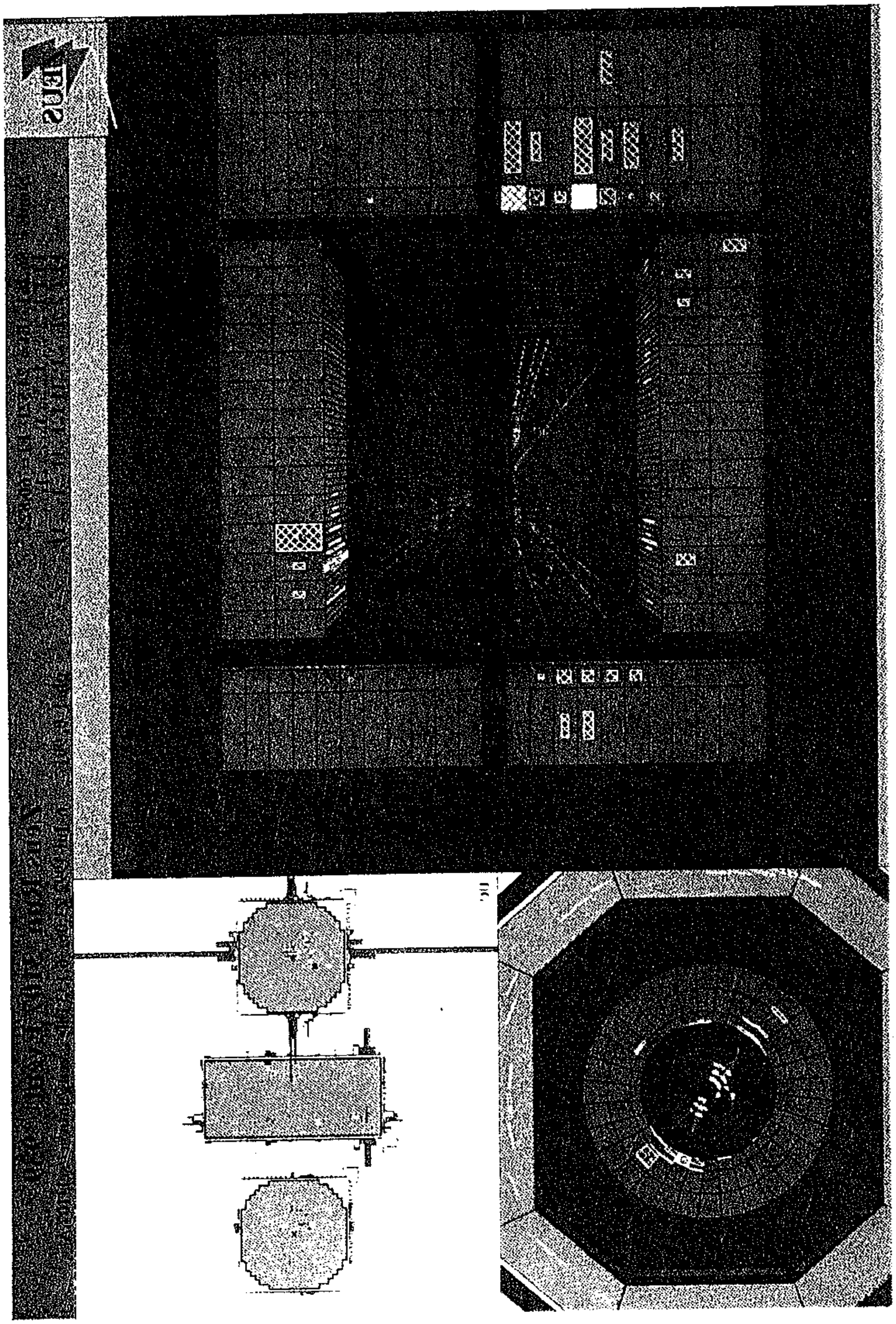

UP SUPERIÉURE OBEN おもて

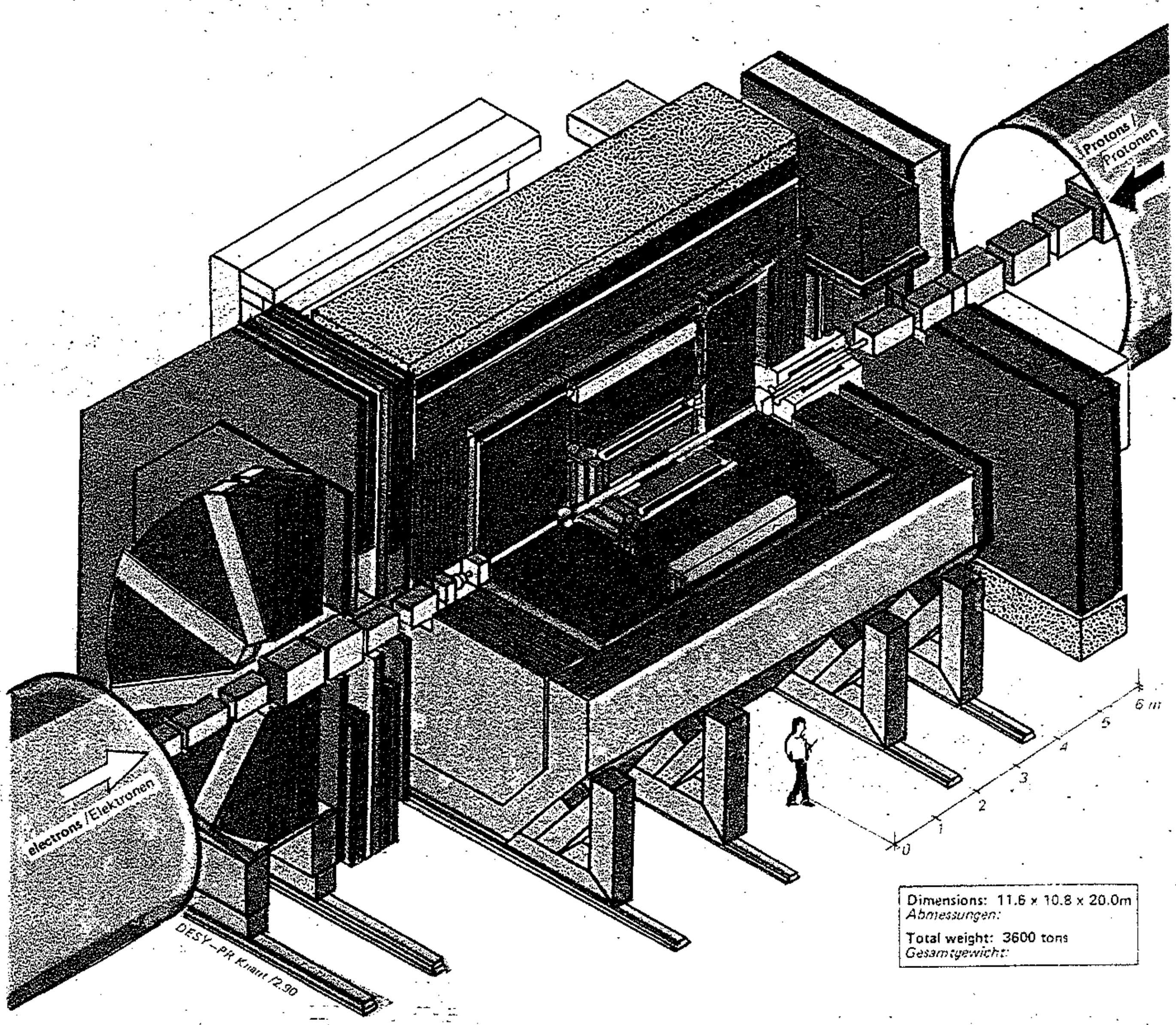

DU-Scintillator Calorimeter
FCAL, BCAL, RCAL
DU-Szintillator-Kalorimeter
FCAL, BCAL, RCAL

Backing Calorimeter,
BAC
Ruckwärts-Kalorimeter
BAC

Vertex Detector
VXD
Vertex-Detektor
VXD

Central Track Detector CTD
Rear Forward Track Detector
FTD, TRD, RTD
Zentrale Spurenkammern CTD
Vorwarts-Spurenkammern
FTD, TRD, RTD

Superconducting Solenoid
and Compensator
Supraleitender Solenoid
und Kompensationsspule

Muon Detector
FMU, BMU, RMU
Myon-Detektor
FMU, BMU, RMU

Muon toroid magnet
Myon-Toroid-Magnet

Concrete Shield
Beton-Abschirmung

HERA Magnets and
Vacuum Chambers
HERA-Magnete
und Vakuumkammern

Iron shielding
Eisen-Abschirmung

Cryo Technics (5)
Kältetechnik (5)

Dimensions: 11.6 x 10.8 x 20.0m
Abmessungen:
Total weight: 3600 tons
Gesamtgewicht:

Experiment ZEUS

Experimental Hall HERA South
Experimentierhalle HERA-Süd

6. SUMMARY

1) EVOLUTION DYNAMICS IS UNDERSTOOD
FOR $\alpha_s \log \frac{Q^2}{\Lambda^2} \ll 1$ (NTLO) & $\alpha_s \ln \frac{1}{x} \ll 1$ (LO)

2) PROBLEMS:
- FACTORIZATION & HIGHER TWISTS
- RECOMBINATION EFFECTS, ONSET: WHERE?
- NONPERTURBATIVE IMPACT ?

3) DIFFERENT POSSIBLE TESTS:
— ACCESS TO xG :
- QCD TEST: F_2
- F_L s_1, s_2; $\sigma_{\text{compt.}}$
- $\sigma_{c\bar{c}}$
- $\sigma_{J/\psi}$, σ_γ

4) COMPARE RESULTS IN THE AP-RANGE
AND THE 'TRUE' SMALL x RANGE

⟶ DISCOVER / BOUND SCREENING EFFECTS
⟶ —"— EFFECTS DUE TO THE LIPATOV EQUATION

5) PERTURBATIVE QCD FOR SMALL x ($x \sim 10^{-4}$, $Q^2 = 10\,\text{GeV}^2$)
IS STILL TO BE WORKED OUT, EVEN IF IT WILL
TURN OUT THAT THE EFFECTS ARE SUBLEADING.

WE DO NOT KNOW YET.

H1
March
93
Moriond